TR 1318

NATIONAL ADVISORY COMMITTEE FOR AERONAUTICS

REPORT 1318

THREE-DIMENSIONAL TRANSONIC FLOW THEORY APPLIED TO SLENDER WINGS AND BODIES

By MAX. A. HEASLET and JOHN R. SPREITER

The Garrett Corporation
AiResearch Mfg. Div.
AUG 28 1975
LIBRARY

1957

For sale by the Superintendent of Documents, U. S. Government Printing Office, Washington 25, D. C. Yearly subscription, $10; foreign, $11.25
single copy price varies according to size - - - - - - - - - Price 35 cents

REPORT 1318

THREE-DIMENSIONAL TRANSONIC FLOW THEORY APPLIED TO SLENDER WINGS AND BODIES

By MAX. A. HEASLET and JOHN R. SPREITER

Ames Aeronautical Laboratory
Moffett Field, Calif.

National Advisory Committee for Aeronautics

Headquarters, 1512 H Street NW., Washington 25, D. C.

Created by Act of Congress approved March 3, 1915, for the supervision and direction of the scientific study of the problems of flight (U. S. Code, title 50, sec. 151). Its membership was increased from 12 to 15 by act approved March 2, 1929, and to 17 by act approved May 25, 1948. The members are appointed by the President and serve as such without compensation.

JAMES H. DOOLITTLE, Sc. D., Shell Oil Company, *Chairman*

LEONARD CARMICHAEL, Ph. D., Secretary, Smithsonian Institution, *Vice Chairman*

ALLEN V. ASTIN, Ph. D., Director, National Bureau of Standards.

PRESTON R. BASSETT, M. A., Vice President, Sperry Rand Corp.

DETLEV W. BRONK, Ph. D., President, Rockefeller Institute for Medical Research.

FREDERICK C. CRAWFORD, Sc. D., Chairman of the Board, Thompson Products, Inc.

WILLIAM V. DAVIS, JR., Vice Admiral, United States Navy, Deputy Chief of Naval Operations (Air).

JEROME C. HUNSAKER, Sc. D., Massachusetts Institute of Technology.

CHARLES J. MCCARTHY, S. B., Chairman of the Board, Chance Vought Aircraft, Inc.

CARL J. PFINGSTAG, Rear Admiral, United States Navy, Assistant Chief for Field Activities, Bureau of Aeronautics.

DONALD L. PUTT, Lieutenant General, United States Air Force, Deputy Chief of Staff, Development.

JAMES T. PYLE, A. B., Administrator of Civil Aeronautics.

FRANCIS W. REICHELDERFER, Sc. D., Chief, United States Weather Bureau.

EDWARD V. RICKENBACKER, Sc. D., Chairman of the Board, Eastern Air Lines, Inc.

LOUIS S. ROTHSCHILD, Ph. B., Under Secretary of Commerce for Transportation.

NATHAN F. TWINING, General, United States Air Force, Chief of Staff.

HUGH L. DRYDEN, PH. D., *Director*

JOHN W. CROWLEY, JR., B. S., *Associate Director for Research*

JOHN F. VICTORY, LL. D., *Executive Secretary*

EDWARD H. CHAMBERLIN, *Executive Officer*

HENRY J. E. REID, D. Eng., Director, Langley Aeronautical Laboratory, Langley Field, Va.

SMITH J. DEFRANCE, D. Eng., Director, Ames Aeronautical Laboratory, Moffett Field, Calif.

EDWARD R. SHARP, Sc. D., Director, Lewis Flight Propulsion Laboratory, Cleveland, Ohio

WALTER C. WILLIAMS, B. S., Chief, High-Speed Flight Station, Edwards, Calif.

CONTENTS

	Page
SUMMARY	1
INTRODUCTION	1
FUNDAMENTAL EQUATIONS AND BOUNDARY CONDITIONS	2
DERIVATION OF INTEGRAL EQUATIONS FOR TRANSONIC FLOW	4
Integral Equation, $M_\infty \leqq 1$	4
Integral Equation, $M_\infty \geqq 1$	6
Calculation of Conditions on Shock Surfaces	7
REDUCTION TO SONIC FLOW THEORY	9
Integrated Strengths of External Sources	9
Integral Equation for Slender Bodies, $M_\infty = 1$	10
SLENDER-WING THEORY IN LINEARIZED FLOW	12
Analysis	12
Evaluation of order of error in equation (62)	14
SLENDER-WING THEORY IN SONIC FLOW	14
Analysis	15
APPLICATIONS TO SEVERAL PROBLEMS INVOLVING SONIC FLOW	16
Resumé of Principal Results of Slender-Body Theory	16
Determination of $g'(x)$ in Terms of Pressure Distribution on a Nonlifting Body of Revolution	18
Relation Between Pressure Distributions on Related Wings and Bodies	19
Wings and bodies having same longitudinal distribution of cross-section area	19
Wings and bodies having similar longitudinal distribution of cross-section area	19
Application to the Calculation of Pressures and Forces on Thin Elliptic Cone-Cylinders at $M_\infty = 1$	20
Pressure distribution on nonlifting cone-cylinders	20
Drag of nonlifting cone-cylinders	20
Pressures and forces on lifting cone-cylinders	22
Momentum Analysis of Drag of Slender Bodies at $M_\infty = 1$	23
Derivation of general relation for drag	23
Relation between drag of wings and bodies having the same area distribution	24
Special cases for which the drag of wing and body is the same	24
Application to Nonplanar Problems	25
Comparison With Experimental Results	26
Cone-cylinders	26
Wings	27
Wing-body combinations	28
REFERENCES	28

REPORT

THREE-DIMENSIONAL TRANSONIC FLOW THEORY APPLIED TO SLENDER WINGS AND BODIES

By Max. A. Heaslet and John R. Spreiter [1]

SUMMARY

The present paper re-examines the derivation of the integral equations for transonic flow around slender wings and bodies of revolution, giving special attention to conditions resulting from the presence of shock waves and to the reduction of the relations to the special forms necessary for the discussion of sonic flow, that is, flow at free-stream Mach number 1. In the vicinity of the body, the disturbance field is then shown to consist of a two-dimensional disturbance field extending laterally and a longitudinal field that depends on the streamwise growth of cross-section area. This result extends Oswatitsch's equivalence rule to lifting cases, provided the angle of attack is small relative to the thickness ratio. The correctness of the analysis is checked by examination of Yoshihara's numerical solution for sonic flow around a slender, circular cone-cylinder and this solution is checked, in turn, by comparison with experimental results of Solomon. An example is presented in which the general result is applied to calculate pressure and integrated forces on a family of slender, elliptic cone-cylinders. An expression is derived which permits the ready calculation of the difference in drag of two slender bodies having the same longitudinal distribution of cross-section area. Classes of wings and bodies are described for which the difference in drag is zero and the Whitcomb area rule applies. Experimental data for such a family of wings of rectangular plan form are examined and it is shown that theory and experiment are in good accord.

INTRODUCTION

The equations governing transonic flows are known and well established by favorable comparisons with experiment (see ref. 1 for a resumé). The difficulties arising as a result of the nonlinearity and mixed character of the differential equation for the potential, however, have prevented the rapid advancement of the analysis such as has occurred in recent years with both subsonic and supersonic theory. This is particularly true for three-dimensional transonic flows and, as a result, perhaps greater than usual effort has gone into the determination and utilization of relations between solutions. The first of these to be advanced was the transonic similarity rule which pertains to the pressures and forces on affinely related wings (refs. 2, 3, and 4) and bodies of revolution (ref. 5). A second relation is the area rule established empirically by Whitcomb (ref. 6) which states that "near the speed of sound, the zero-lift drag rise of thin low-aspect-ratio wing-body combinations is primarily dependent on the axial distribution of cross-sectional area normal to the air stream." A third relation is the equivalence rule of Oswatitsch (refs. 7 and 8) which may be stated as follows: "The solution for transonic flow around a thin, nonlifting, low-aspect-ratio wing can be obtained from that for a nonlifting body of revolution having the same longitudinal distribution of cross-sectional area by superposing the difference between the two-dimensional harmonic cross-flow solutions for the two bodies." The area rule and the equivalence rule are, obviously, closely related. Further effort needs to be expended, however, in establishing the generality and range of validity of these relations and in exploiting the results in specific applications. The present paper is concerned with this task.

The problem will be approached through application of the classical method of singularities. This is one of the oldest and most fruitful methods for solving partial differential equations and has reached a high state of development in linearized compressible-flow theory. There is also a considerable body of literature in which the method is applied to nonlinear compressible-flow problems by considering the solution of the linearized equations to be a first approximation, and iterating to obtain second and higher order approximations. The results so calculated are good approximations to pure subsonic flows or to pure supersonic flows, but it is now generally agreed that the series representation of the solution does not converge in the transonic range. Approximate calculations by Oswatitsch (refs. 9 and 10) have indicated the possibility, however, that the method of singularities might be applied successfully in the transonic range if the idea is relinquished that the linear solution is necessarily the first approximation in the transonic range. This idea has been pursued further in references 11 through 15 in which a number of improvements are introduced and the results of numerous specific calculations are shown. Although the basic equations are derived for three-dimensional flow in the latter references, all applications are to two-dimensional flows. The values of the free-stream Mach number, moreover, are restricted to values no greater than unity.

[1] Supersedes NACA TN 3717 by Max. A. Heaslet and John R. Spreiter.

The same general approach has been applied to three-dimensional transonic flow around slender wings and bodies by Oswatitsch and Keune (ref. 8) and by Harder and Klunker (ref. 16). In these applications, the principal aim is not to determine actual solutions but to derive relations between solutions for various bodies having the same longitudinal distribution of cross-section area. These two analyses are not entirely satisfactory in a number of particulars, not the least of which is the omission of all considerations of shock waves in the body of the analysis. A more important, although perhaps more subtle, point concerns the treatment of the cumulative effect of the nonlinear term of the transonic equation when the free-stream Mach number M_∞ is unity. Harder and Klunker argue that the effect on the induced flow field is small because the term itself is everywhere small. Actually, however, the cumulative effect of this term leads to infinite contributions at $M_\infty=1$. Oswatitsch and Keune consider the cumulative effect but circumvent the difficulty by introducing rather arbitrarily selected values for Mach number so chosen that the value of unity is never inserted into the vital integrals. It is the initial concern of the present analysis, therefore, to re-examine the derivation of the integral equations for transonic flow around slender wings and bodies of revolution, giving special attention to conditions resulting from the presence of shock waves and to the reduction of the relations to the special forms necessary for sonic flow. In contrast to references 8 through 15, which are concerned exclusively with cases in which the free-stream Mach number is no greater than unity, equations are also derived herein for the case where the free stream is supersonic. These equations are likewise reduced to the special form associated with sonic flow and the results are shown to be identical to those which arise from a consideration of flows with a subsonic free-stream velocity.

Following the establishment of the basic integral relations for transonic flow, special attention is directed toward the case where the free-stream Mach number is unity. Here, the integral relations are simpler in character, although still nonlinear. Application of a convergent interation process leads to the conclusion that the solution for the potential has a particularly simple form in the vicinity of the body; in common with linearized slender-body theory, the disturbance field consists, to a given order of error, of a two-dimensional disturbance field extending laterally and a longitudinal field that depends on the streamwise growth of cross-sectional area. This result extends Oswatitsch's equivalence rule to lifting cases, provided the angle of attack is small relative to the thickness ratio. The correctness of the analysis is checked by examination of Yoshihara's numerical solution for sonic flow around a slender, circular, cone-cylinder given in reference 17, and this solution is checked, in turn, by comparison with experimental results of Solomon given in reference 18. The results yield a simple means of determining the pressure distribution on an entire family of slender wings and bodies having the same longitudinal distribution of cross-sectional area when the pressure distribution is known for any member of the family. Starting with the known solution for the circular cone-cylinder, an example is presented in which the general result is applied to a family of slender elliptic cone-cylinders. This example, which was discussed briefly in reference 1, is examined in detail. It is shown that the lift and the load distribution are the same as given by linear theory, confirming the ideas advanced in reference 19. Contrary to Whitcomb's area rule, however, the drag depends significantly on the cross-section shape. Both the drag and lift of the thin elliptic cone-cylinder are shown to be in accord with the transonic similarity rules. A momentum analysis of the sonic drag of slender bodies in general is then undertaken and an expression is derived which permits the ready calculation of the difference in drag of two slender bodies having the same longitudinal distribution of cross-section area. This result confirms the drag variation calculated for the elliptic cone-cylinders by integration of the surface pressures. Several large and significant classes of wings and bodies are described for which the difference in drag is zero and the Whitcomb area rule applies without modification. One of these is a family of affinely related wings. Experimental data from reference 20 for such a family of wings of rectangular plan form are examined and it is shown that theory and experiment are in good accord, provided the product of aspect ratio and cube root of the thickness ratio is, in this instance, less than about unity.

The final section of the report has been written so as to be as self-contained as possible and readers concerned solely with applications of the theory may find this section sufficient for their purposes. The initial sections of the report have been written for readers concerned with a more complete understanding of the derivation and limitations of the general theory together with the evaluation of the order of error incurred in the slender-body approximation.

FUNDAMENTAL EQUATIONS AND BOUNDARY CONDITIONS

The basic equations necessary for the discussion of inviscid transonic flow consist of a set of partial differential equations relating the velocity components and their gradients at every point, together with an auxiliary relation for the velocity jump through a shock wave. For thin wings and slender bodies inclined at zero or small angles of attack, the differential equations can be simplified if the shock waves are assumed sufficiently weak that the flow is irrotational and isentropic, thereby permitting the introduction of a velocity potential Φ. The further assumption of small disturbances leads to the use of a perturbation velocity potential φ which in Cartesian coordinates satisfies the following nonlinear partial differential equation

$$(1-M_\infty^2)\varphi_{xx}+\varphi_{yy}+\varphi_{zz}=M_\infty^2\frac{\gamma+1}{U_\infty}\varphi_x\varphi_{xx} \tag{1}$$

where U_∞ and M_∞ refer to the velocity and Mach number of the undisturbed flow, γ is the ratio of specific heats ($\gamma=1.4$ for air), and x, y, and z are Cartesian coordinates. The perturbation velocity vector is given by the gradient of φ and has components, u, v, and w along the three axes.

Knowledge of methods for obtaining solutions of equation (1) is meager not only because it is nonlinear, but because it changes type (elliptic, parabolic, hyperbolic). This change of type is an essential feature of transonic flow, since subsonic flows are represented by elliptic equations and supersonic flows

by hyperbolic equations. If both types of flow occur in a single flow field, it is apparent that the differential equation must change type. In the present case, the type of the equation is recognized by the sign of the total coefficient of φ_{xx}, as follows

$$(1-M_\infty^2)-M_\infty^2(\gamma+1)\frac{\varphi_x}{U_\infty}\begin{cases}>0 \text{ elliptic (subsonic)}\\ =0 \text{ parabolic (sonic)}\\ <0 \text{ hyperbolic (supersonic)}\end{cases} \tag{2}$$

In most of the investigations of two-dimensional transonic flows ($\varphi_{yy}=0$), the differential equation is transformed into a linear equation of mixed type (Tricomi equation) by the introduction of the hodograph variables. At the present time, however, no transformation is known that achieves a corresponding linearization of the three-dimensional equation, and the investigation of other methods of solution thus becomes relatively more important.

Equation (1) is, of course, valid only in regions where the necessary derivatives exist and are continuous. Since these conditions do not hold where shock waves occur, and since shock waves are a prominent feature of most transonic flows, an additional equation is needed for the transition through the shock. The fundamental properties of a shock surface require that the normal component of velocity be discontinuous and the tangential component, and therefore φ, be continuous. The necessary relation follows from the classical expression for the shock polar, which in the small disturbance transonic theory is approximated by

$$(1-M_\infty^2)(\varphi_{x_a}-\varphi_{x_b})^2+(\varphi_{y_a}-\varphi_{y_b})^2+(\varphi_{z_a}-\varphi_{z_b})^2$$
$$=M_\infty^2\frac{\gamma+1}{U_\infty}\frac{\varphi_{x_a}+\varphi_{x_b}}{2}(\varphi_{x_a}-\varphi_{x_b})^2 \tag{3}$$

where the subscripts a and b refer to conditions ahead of the behind the shock.

Equations (1) and (3) are usually developed for the case where the coordinate system is placed so that the x axis is parallel to the undisturbed stream at infinity, but they also apply to the case where the coordinate system is rotated slightly. In the present analysis, it is convenient to aline the x axis with the longitudinal axis of the wing or body as shown in figure 1. Such a system is usually referred to as the body axes. With these coordinates, the relation between the total velocity potential $\Phi(x,y,z)$ and the perturbation velocity potential $\varphi(x,y,z)$ is approximated by

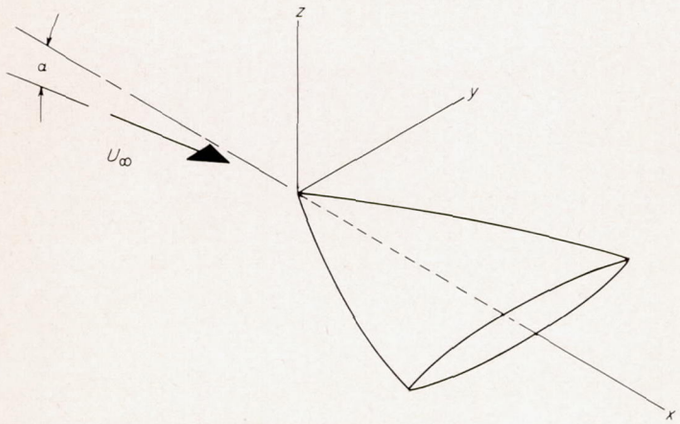

FIGURE 1.—View of wing and coordinate system.

$$\Phi(x,y,z,)=U_\infty(x+\alpha z)+\varphi(x,y,z) \tag{4}$$

where α is the angle of attack.

The expression for the pressure coefficient C_p is not invariant with respect to small rotations of the coordinate system. In body axes, the proper expression is

$$C_p=-\frac{2}{U_\infty}(\varphi_x+\alpha\varphi_z)-\frac{1}{U_\infty^2}(\varphi_y^2+\varphi_z^2) \tag{5}$$

The boundary conditions require that the gradient of the total velocity potential evaluated infinitely far from the aircraft be consistent with the uniform free-stream conditions there and, when evaluated normal to and on the surface of the airplane itself, be zero. The condition at infinity yields $\Phi(\infty)=U_\infty(x+\alpha z)$ or that

$$\varphi(\infty)=0 \tag{6}$$

An exception to this statement occurs in the vicinity of the wake at great distances behind the wing, but no complication ensues due to the relative smallness of this region. The condition at the airplane surface results in the relation

$$\frac{\partial\Phi}{\partial\tilde{n}}\equiv U_\infty(n_1+\alpha n_3)+n_1\frac{\partial\varphi}{\partial x}+n_2\frac{\partial\varphi}{\partial y}+n_3\frac{\partial\varphi}{\partial z}=0 \tag{7}$$

where n_1, n_2, and n_3 are the direction cosines of a normal to the airplane surface with respect to the x, y, and z axes, respectively. This relation is too general for the present needs, however, because it applies to all shapes, whereas the analysis is to be a small disturbance theory that applies only to slender bodies and thin wings. For such configurations, n_1 is small nearly everywhere on the surface and will be neglected in comparison with either unity or $(n_2^2+n_3^2)^{1/2}$. In this way, equation (7) simplifies to

$$U_\infty(n_1+\alpha n_3)+n_2\frac{\partial\varphi}{\partial y}+n_3\frac{\partial\varphi}{\partial z}=U_\infty(n_1+\alpha n_3)+\frac{\partial\varphi}{\partial n}=0 \tag{8}$$

where n is the normal to the curve bounding a cross section in a plane normal to the x axis.

All of the subsequent analysis proceeds from Green's theorem which relates a volume integral over a region V to a surface integral over the surface Σ enclosing V. Green's theorem can be expressed in many ways; here it is found convenient to use the forms associated with the linear differential equation obtained by equating the left-hand member of equation (1) to zero. This results in two different forms of Green's theorem, one for $M_\infty\leqq 1$, and the other for $M_\infty\geqq 1$ and prompts the introduction of the following abbreviations

$$\beta=(|1-M_\infty^2|)^{1/2},\ k=M_\infty^2\frac{\gamma+1}{U_\infty} \tag{9}$$

If the undisturbed flow at infinity is subsonic (i. e., $M_\infty\leqq 1$), equation (1) can be rewritten as

$$\beta^2\varphi_{xx}+\varphi_{yy}+\varphi_{zz}=k\varphi_x\varphi_{xx}=k\frac{\partial}{\partial x}\left(\frac{\varphi_x^2}{2}\right) \tag{10}$$

and the corresponding expression of Green's theorem is (see, e. g., ref. 21)

$$\iiint_V [\psi L(\Omega)-\Omega L(\psi)]\,dV=-\iint_\Sigma\left(\psi\frac{\partial\Omega}{\partial\nu}-\Omega\frac{\partial\psi}{\partial\nu}\right)d\Sigma \tag{11}$$

where Ω and ψ are arbitrary functions and $L(\Omega)$ is defined as follows

$$L(\Omega)\equiv\beta^2\Omega_{xx}+\Omega_{yy}+\Omega_{zz} \tag{12}$$

and $\partial\Omega/\partial\nu$ is a derivative along the conormal and is defined by

$$\frac{\partial\Omega}{\partial\nu}\equiv\frac{\partial\Omega}{\partial x}\beta^2 n_1+\frac{\partial\Omega}{\partial y}n_2+\frac{\partial\Omega}{\partial z}n_3 \tag{13}$$

where n_1, n_2, n_3 are the direction cosines of the normal to the surface drawn into the region V.

If the undisturbed flow at infinity is supersonic (i. e., $M_\infty\geqq 1$), equation (1) can be written as

$$-\beta^2\varphi_{xx}+\varphi_{yy}+\varphi_{zz}=k\varphi_x\varphi_{xx}=k\frac{\partial}{\partial x}\left(\frac{\varphi_x^2}{2}\right) \tag{14}$$

and the corresponding expression of Green's theorem is

$$\iiint_{\overline{V}} [\psi\overline{L}(\Omega)-\Omega\overline{L}(\psi)]\,d\overline{V}=-\iint_{\overline{\Sigma}}\left(\psi\frac{\partial\Omega}{\partial\overline{\nu}}-\Omega\frac{\partial\psi}{\partial\overline{\nu}}\right)d\overline{\Sigma} \tag{15}$$

where the following definitions

$$\overline{L}(\Omega)\equiv-\beta^2\Omega_{xx}+\Omega_{yy}+\Omega_{zz} \tag{16}$$

and

$$\frac{\partial\Omega}{\partial\overline{\nu}}=-\frac{\partial\Omega}{\partial x}\beta^2 n_1+\frac{\partial\Omega}{\partial y}n_2+\frac{\partial\Omega}{\partial z}n_3 \tag{17}$$

apply.

DERIVATION OF INTEGRAL EQUATIONS FOR TRANSONIC FLOW

In this section, integral equations corresponding to the transonic differential equation are derived for subsonic and supersonic free-stream conditions. One of the principal contributions here evolves from the attention given to the shock waves, or discontinuity surfaces, appearing in the flow fields. It will appear (see eqs. (23) and (30)) that the perturbation velocity potential can be expressed, for M_∞ less than or greater than 1, as the sum of integrals that show no explicit contribution of the shocks. Closer analysis of these integrals reveals, however, that discontinuities in velocity can appear and that they automatically satisfy the shock-polar relations (see eqs. (34) and (37)). This section is prefatory to the formulation of the transonic integral equations for the particular cases of a slender body of revolution and a thin wing.

INTEGRAL EQUATION, $M_\infty\leqq 1$

The function ψ in Green's theorem, equation (11), is now identified with the fundamental solution $1/\sigma$ of the differential equation $L(\psi)=0$ and the function φ is replaced by Ω, the perturbation velocity potential of the flow field under consideration. From equations (10) and (11), the following relations hold

$$\iint_\Sigma\left(\frac{1}{\sigma}\frac{\partial\varphi}{\partial\nu}-\varphi\frac{\partial}{\partial\nu}\frac{1}{\sigma}\right)d\Sigma=-\iiint_V\frac{1}{\sigma}L(\varphi)dV$$

$$=-\iiint_V\frac{k}{\sigma}\frac{\partial}{\partial x_1}\left(\frac{\varphi_{x_1}^2}{2}\right)dV \tag{18}$$

where

$$\sigma=[(x-x_1)^2+\beta^2(y-y_1)^2+\beta^2(z-z_1)^2]^{1/2} \tag{19}$$

In these equations the running coordinates in the integrations are x_1, y_1, and z_1 and φ is to be calculated at a point P with coordinates x, y, and z.

Equation (18) is now applied to the infinite region V surrounding the given object to be studied. Some care must be exercised, however, in fixing the enclosing surface Σ since Green's theorem requires that singularities and regions of discontinuity must be excluded from the domain of integration. It is to be noted, first, that σ vanishes at $x=x_1$, $y=y_1$, and $z=z_1$ and the effect of the resultant singularity can be determined only after the field point is enclosed by a neighboring surface and the region V taken external to this surface. Second, since shock waves are to be expected within the flow field and discontinuities in the perturbation velocity components occur across these waves, the boundary of V must also be drawn so as to exclude such discontinuity surfaces.

In figure 2, a schematic indication of the body and the region of integration is shown. The complete three-dimensional extent of the body has not been pictured; it suffices, however, to state that the surface Σ (shown dashed) is composed of a sphere of large radius which forms the external boundary of V, a sphere of infinitesimal radius surrounding the field point P, and a final surface enveloping the object, its wake, and its shock waves.

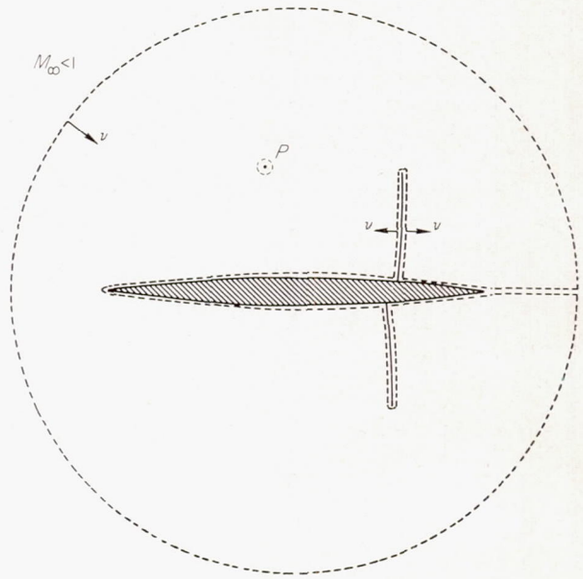

FIGURE 2.—Region of integration; $M_\infty\leqq 1$.

If equation (18) is applied to this region and the a priori assumption is made that the perturbation field attenuates sufficiently fast with distance to negate the contribution of the surface integral over the large sphere in the limit as the radius goes to infinity, the following expression results:

$$\varphi(x,y,z)=-\frac{1}{4\pi}\iint_{O+W}\left(\frac{1}{\sigma}\frac{\partial\sigma}{\partial\nu}-\varphi\frac{\partial}{\partial\nu}\frac{1}{\sigma}\right)d\Sigma-\frac{1}{4\pi}\iint_{\lambda_a}\left(\frac{1}{\sigma}\frac{\partial\varphi}{\partial\nu}-\varphi\frac{\partial}{\partial\nu}\frac{1}{\sigma}\right)d\Sigma-\frac{1}{4\pi}\iint_{\lambda_b}\left(\frac{1}{\sigma}\frac{\partial\varphi}{\partial\nu}-\varphi\frac{\partial}{\partial\nu}\frac{1}{\sigma}\right)d\Sigma-\frac{k}{4\pi}\iiint_V\frac{1}{\sigma}\frac{\partial}{\partial x_1}\frac{\varphi_{x_1}^2}{2}dV \quad (20)$$

In this equation, the integration region over the surface of the object and its wake is denoted by $O+W$. The derivatives in the surface integrals are, in all cases, along lines directed away from the integration surface and into the three-dimensional domain V since, as follows from equation (13), the direction numbers have the same sign as the direction numbers of the true normal and the Mach number effect is limited to a foreshortening of the longitudinal dimension. On the shock surface λ the conormals are directly opposed on the upstream and downstream faces λ_a and λ_b. On the body itself, the conormal derivative can be simplified in the manner used in developing the boundary conditions of equations (8); that is, from the restrictions imposed on the gradients along the body surface, the direction of the conormal becomes effectively that of the normal n lying in the crossplanes $x_1=\text{const}$. Thus

$$\frac{\partial}{\partial\nu}\approx n_2\frac{\partial}{\partial y}+n_3\frac{\partial}{\partial z}=\frac{\partial}{\partial n}$$

on the surface of the body and wake.

If the triple (spatial) integral of equation (20) is integrated by parts x-wise, the resultant form is

$$\varphi(x,y,z)=-\frac{1}{4\pi}\iint_{O+W}\left[\frac{1}{\sigma}\left(\frac{\partial\varphi}{\partial n}-\frac{k}{2}\varphi_{x_1}^2n_1\right)-\varphi\frac{\partial}{\partial n}\frac{1}{\sigma}\right]d\Sigma-\frac{1}{4\pi}\iint_{\lambda_a}\left[\frac{1}{\sigma}\left(\frac{\partial\varphi}{\partial\nu}-\frac{k}{2}\varphi_{x_1}^2n_1\right)-\varphi\frac{\partial}{\partial\nu}\frac{1}{\sigma}\right]d\Sigma-\frac{1}{4\pi}\iint_{\lambda_b}\left[\frac{1}{\sigma}\left(\frac{\partial\varphi}{\partial\nu}-\frac{k}{2}\varphi_{x_1}^2n_1\right)-\varphi\frac{\partial}{\partial\nu}\frac{1}{\sigma}\right]d\Sigma+\frac{k}{4\pi}\iiint_V\frac{1}{2}\varphi_{x_1}^2\left(\frac{\partial}{\partial x_1}\frac{1}{\sigma}\right)dV \quad (21)$$

Equation (21) is of particular interest because the integrals over the shock surfaces may be shown to vanish. In order to prove this, one notes first that the two integrals extend over the same geometric surface but that the integrands are evaluated, respectively, on the upstream and downstream faces and, by definition, the directions of the conormals are opposed. When the integrands are combined, the total integrand can be expressed as the difference of the two terms, one of which contains the factor $(\varphi)_{\lambda_b}-(\varphi)_{\lambda_a}$ and the other contains the factor

$$\left(\varphi_{x_1}\beta^2n_1+\varphi_{y_1}n_2+\varphi_{z_1}n_3-\frac{k}{2}\varphi_{x_1}^2n_1\right)_{\lambda_a}+\left(\varphi_{x_1}\beta^2n_1+\varphi_{y_1}n_2+\varphi_{z_1}n_3-\frac{k}{2}\varphi_{x_1}^2n_1\right)_{\lambda_b}$$

The first of these factors vanishes by virtue of the fact noted previously that the perturbation potential is continuous across a shock surface. The second factor can be rewritten in the form

$$\beta^2(u_{\lambda_b}-u_{\lambda_a})(n_1)_{\lambda_b}+(v_{\lambda_b}-v_{\lambda_a})(n_2)_{\lambda_b}+(w_{\lambda_b}-w_{\lambda_a})(n_3)_{\lambda_b}-\frac{k}{2}(u_{\lambda_b}^2-u_{\lambda_a}^2)(n_1)_{\lambda_b}$$

Also, the change in the velocity vector occurring at the shock surface must be in a direction normal to the shock. This implies the relations

$$(n_1)_{\lambda_b}:(n_2)_{\lambda_b}:(n_3)_{\lambda_b}=(u_{\lambda_b}-u_{\lambda_a}):(v_{\lambda_b}-v_{\lambda_a}):(w_{\lambda_b}-w_{\lambda_a})$$

Thus, the second factor to be evaluated becomes

$$\frac{\beta^2(u_{\lambda_b}-u_{\lambda_a})^2+(v_{\lambda_b}-v_{\lambda_a})^2+(w_{\lambda_b}-w_{\lambda_a})^2-\frac{k}{2}(u_{\lambda_b}^2-u_{\lambda_a}^2)(u_{\lambda_b}-u_{\lambda_a})}{[(u_{\lambda_b}-u_{\lambda_a})^2+(v_{\lambda_b}-v_{\lambda_a})^2+(w_{\lambda_b}-w_{\lambda_a})^2]^{1/2}}$$

The numerator of this fraction, however, corresponds to the shock-polar conditions of equation (3) and the expression vanishes.

It finally remains to remark that in the surface integral over the body itself, the term $n_1\varphi_{x_1}^2$ resulting from the integration by parts is of higher order than the normal derivative of the perturbation potential. The term can therefore be neglected and equation (21) becomes

$$\varphi(x,y,z)=-\frac{1}{4\pi}\iint_{O+W}\left(\frac{1}{\sigma}\frac{\partial\varphi}{\partial n}-\varphi\frac{\partial}{\partial n}\frac{1}{\sigma}\right)d\Sigma+\frac{k}{4\pi}\iiint_V\frac{1}{2}\varphi_{x_1}^2\left(\frac{\partial}{\partial x_1}\frac{1}{\sigma}\right)dV \quad (22)$$

Equation (22) provides another integral expression for the perturbation velocity potential, for $M_\infty\leqq 1$, in transonic flow theory. The first integral on the right is algebraically equivalent to the expression for $\varphi(x, y, z)$ in linearized theory and the spatial integral is a contribution brought about by the nonlinear term of the basic differential equation. It is of interest to remark that a derivation ignoring the existence of the shock waves can also lead to the same form of the equation. In this respect the relation is not unlike cases arising in linearized supersonic theory where it becomes necessary to study the contribution provided by the foremost shock wave induced by the body. For the majority of cases of practical interest, it can be shown that compensating terms arise and that the discontinuity surfaces are taken care of by a formal development that ignores the existence of these surfaces (see, e. g., refs. 22 and 23). It is not possible, however, to ignore so completely the existence of the discontinuity surface in transonic flow and, as will be seen in the later developments, equation (20) is, for certain purposes, preferable to equation (22).

Equations (20) and (22) will now be written, for purposes of reference, in the following final forms

$$\varphi(x,y,z)=\varphi_L(x,y,z)+\frac{k}{4\pi}\iiint_V \frac{1}{2}\varphi_{x_1}{}^2\left(\frac{\partial}{\partial x_1}\frac{1}{\sigma}\right)dV \tag{23a}$$

$$=\varphi_L(x,y,z)-\frac{k}{4\pi}\frac{\partial}{\partial x}\iiint_V \frac{1}{2}\varphi_{x_1}{}^2\frac{1}{\sigma}dV \tag{23b}$$

$$=\varphi_L(x,y,z)-\frac{1}{4\pi}\iint_\lambda \Delta\left(\frac{\partial\varphi}{\nu}\right)\frac{1}{\sigma}d\Sigma-\frac{k}{4\pi}\iiint_V\left(\frac{\partial}{\partial x_1}\frac{\varphi_{x_1}{}^2}{2}\right)\frac{1}{\sigma}dV \tag{23c}$$

$$=\varphi_L(x,y,z)-\frac{1}{4\pi}\frac{\partial}{\partial x}\iint_\lambda \Delta\left(\frac{\partial\varphi}{\partial\nu}\right)\omega d\Sigma-\frac{k}{4\pi}\frac{\partial}{\partial x}\iiint\left(\frac{\partial}{\partial x_1}\frac{\varphi_{x_1}{}^2}{2}\right)\omega dV \tag{23d}$$

In each of the above equations, φ_L has the analytic representation it has in linear theory. The first two relations are obvious repetitions of equation (22). The two latter relations are transcriptions of equation (20) where the notation $\Delta(\partial\varphi/\partial v)=(\partial\varphi/\partial\nu)_{\lambda_a}+(\partial\varphi/\partial\nu)_{\lambda_b}$ has been introduced, the continuity of φ at the shock surface has been used, and where in equation (23d) the variable

$$\omega=\sinh^{-1}\frac{x-x_1}{\beta[(y-y_1)^2+(z-z_1)^2]^{1/2}}$$

$$=\frac{(x-x_1)}{|x-x_1|}\,ln\,\frac{|x-x_1|+\{(x-x_1)^2+\beta^2[(y-y_1)^2+(z-z_1)^2]\}}{\beta[(y-y_1)^2+(z-z_1)^2]^{1/2}}$$

is employed to express the integral equation in a form that will be of value in establishing a reduction to the case of sonic flow.

The longitudinal perturbation velocity is given by the x-wise derivative of any of equations (23). Consider, for example, equation (23a). After first isolating the singularity at the field point by introducing the limits $x_1=x\pm\epsilon$, one has

$$u(x,y,z)$$

$$=\frac{\partial}{\partial x}\varphi_L(x,y,z)+\lim_{\epsilon\to 0}\frac{k}{4\pi}\frac{\partial}{\partial x}\iint dy_1dz_1\left[\int_{-\infty}^{x-\epsilon}\frac{1}{2}\varphi_{x_1}{}^2\left(\frac{\partial}{\partial x_1}\frac{1}{\sigma}\right)dx_1+\int_{x+\epsilon}^{\infty}\frac{1}{2}\varphi_{x_1}{}^2\left(\frac{\partial}{\partial x_1}\frac{1}{\sigma}\right)dx_1\right]=u_L(x,y,z)+$$

$$\lim_{\epsilon\to 0}\frac{k}{2\pi}\iint\frac{1}{2}\varphi_{x_1}{}^2(x;y_1,z_1)\frac{\epsilon dy_1dz_1}{[\epsilon^2+\beta^2(y-y_1)^2+\beta^2(z-z_1)^2]^{3/2}}-\frac{k}{4\pi}\iiint_V\frac{1}{2}\varphi_{x_1}{}^2\left(\frac{\partial^2}{\partial x_1{}^2}\frac{1}{\sigma}\right)dV$$

In the limit as $\epsilon\to 0$ the influence function in the integrand of the double integral is effectively a two-dimensional pulse function at the point $y_1=y$, $z_1=z$ and of strength $2\pi/\beta^2$. The expression for u then becomes

$$u(x,y,z)=u_L(x,y,z)+\frac{k}{\beta^2}\frac{u^2(x,y,z)}{2}-\frac{k}{4\pi}\iiint_V\frac{u^2}{2}\left(\frac{\partial^2}{\partial x_1{}^2}\frac{1}{\sigma}\right)dV \tag{24}$$

A detailed account of the application of the two-dimensional form of this equation to the calculation of airfoil pressure distributions has been given by Spreiter and Alksne (ref. 15).

INTEGRAL EQUATION, $M_\infty \geqq 1$

Use is now made of Green's theorem as expressed in equation (15) and Ω is set equal to the perturbation velocity potential $\varphi(x,y,z)$. The direct analogue of the derivation in the previous section would require that ψ be replaced by $[(x-x_1)^2-\beta^2(y-y_1)^2-\beta^2(z-z_1)^2]^{1/2}$ but this leads to the immediate introduction of a finite-part technique in the integration. For the initial stages of the analysis, ψ will be identified with the fundamental solution $\bar{\omega}$ of $\bar{L}(\psi)=0$ used by Volterra (ref. 24). From equations (14) and (15), the following relations hold:

$$\iint_{\bar\Sigma}\left(\bar{\omega}\frac{\partial\varphi}{\partial\bar{v}}-\varphi\frac{\partial}{\partial\bar{v}}\bar{\omega}\right)d\bar{\Sigma}=-\iiint_{\bar V}\bar{\omega}\bar{L}(\varphi)d\bar{V}$$

$$=-\iiint_{\bar V}k\bar{\omega}\frac{\partial}{\partial x_1}\left(\frac{\varphi_{x_1}{}^2}{2}\right)d\bar{V} \tag{25}$$

where

$$\bar{\omega}=\cosh^{-1}\frac{x-x_1}{\beta[(y-y_1)^2+(z-z_1)^2]^{1/2}}$$

The successful application of equation (25) to the transonic problem hinges on the proper choice of the three-dimensional region $\bar{V}$ and its enclosing surface $\bar{\Sigma}$. Discontinuities in the velocity components are again to be taken into consideration at the shock waves. Furthermore, the fundamental solution of Volterra becomes infinite at $y_1=y$, $z_1=z$, that is, everywhere along the line passing through the field point P and parallel to the x axis. Figure 3 indicates the disturbance field of the object as well as $\bar{V}$ and $\bar{\Sigma}$ (shown with dashed

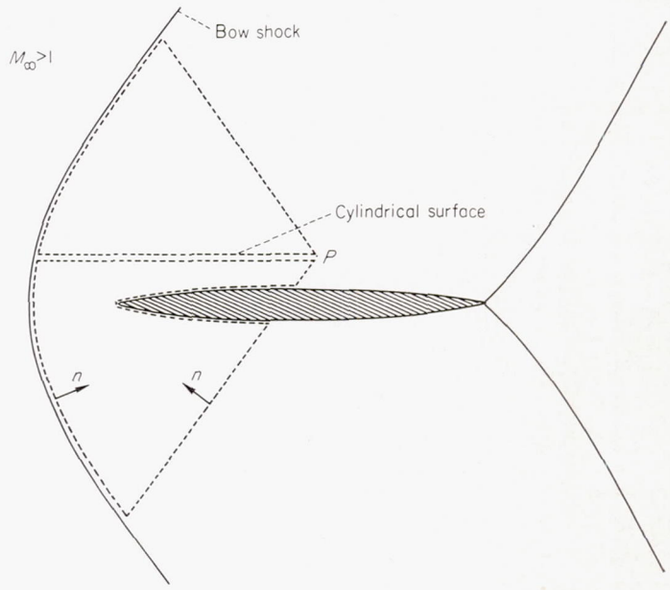

FIGURE 3.—Region of integration; $M_\infty \geqq 1$.

lines). The bow shock fixes the foremost extent to the disturbance field and $\bar{\Sigma}$ lies adjacent to it and other possible shock surfaces as well as the surface of the object and its wake. The downstream limits of the region $\bar{V}$ are fixed by the forecone with vertex at P and determined explicitly by the relation

$$(x-x_1)=\beta[(y-y_1)^2+(z-z_1)^2]^{1/2} \tag{26}$$

The inner boundary of V is the cylindrical surface of infinitesimal radius given by the relation

$$(y-y_1)^2+(z-z_1)^2=\epsilon^2$$

The conormal derivative is defined by equation (17); on the infinitesimal cylinder its direction is parallel to that of the normal to the surface, and on the forecone from P the conormal is directed along the surface itself. Formal analysis yields the expression

$$\begin{aligned}\varphi(x,y,z)=&-\frac{1}{2\pi}\frac{\partial}{\partial x}\iint\left(\bar{\omega}\frac{\partial\varphi}{\partial\bar{\nu}}-\varphi\frac{\partial}{\partial\bar{\nu}}\bar{\omega}\right)d\bar{\Sigma}-\\&\frac{1}{2\pi}\frac{\partial}{\partial x}\iint_{\lambda_a}\left(\bar{\omega}\frac{\partial\varphi}{\partial\bar{\nu}}-\varphi\frac{\partial}{\partial\bar{\nu}}\bar{\omega}\right)d\bar{\Sigma}-\frac{1}{2\pi}\frac{\partial}{\partial x}\iint_{\lambda_b}\left(\bar{\omega}\frac{\partial\varphi}{\partial\bar{\nu}}-\right.\\&\left.\varphi\frac{\partial}{\partial\bar{\nu}}\bar{\omega}\right)d\bar{\Sigma}-\frac{k}{2\pi}\frac{\partial}{\partial x}\iiint_{\bar{V}}\bar{\omega}\frac{\partial}{\partial x_1}\frac{\varphi_{x_1}^2}{2}d\bar{V}\end{aligned} \tag{27}$$

where integrals over the surface of the body and wake are denoted by τ, over the two sides of the shock surfaces by λ_a and λ_b, and over the enclosed volume by $\bar{V}$. In each case, only that portion of the surface or volume lying within the forecone of P is included in the integrals. The surface integrals over the forecone itself vanish because $\bar{\omega}$ and $\partial\bar{\omega}/\partial\bar{\nu}$ are zero. It should be noted that the forecone is that of linearized theory and has no rela ionship to the region of dependence in the actual flow field.

Integration by parts, in the last integral, leads to the relation

$$\begin{aligned}\varphi(x,y,z)=&-\frac{1}{2\pi}\frac{\partial}{\partial x}\iint_{\tau}\left[\bar{\omega}\left(\frac{\partial\varphi}{\partial n}-\frac{k}{2}\varphi_{x_1}^2n_1\right)-\varphi\frac{\partial}{\partial n}\bar{\omega}\right]d\bar{\Sigma}-\\&\frac{1}{2\pi}\frac{\partial}{\partial x}\left(\iint_{\lambda_a}+\iint_{\lambda_b}\right)\left[\bar{\omega}\left(\frac{\partial\varphi}{\partial\bar{\nu}}-\frac{k}{2}\varphi_{x_1}^2n_1\right)-\varphi\frac{\partial}{\partial\bar{\nu}}\bar{\omega}\right]d\bar{\Sigma}+\\&\frac{k}{2\pi}\frac{\partial}{\partial x}\iiint_{\bar{V}}\frac{1}{2}\varphi_{x_1}^2\left(\frac{\partial}{\partial x_1}\bar{\omega}\right)d\bar{V}\end{aligned} \tag{28}$$

Equation (28) is the form, for $M_\infty \geqq 1$, analogous to equation (21), for $M_\infty \leqq 1$, and on the body and wake surfaces involves the approximation

$$\frac{\partial}{\partial\bar{\nu}}\approx n_2\frac{\partial}{\partial y}+n_3\frac{\partial}{\partial z}\approx\frac{\partial}{\partial n}$$

It is not difficult to show, from the shock-wave relation of equation (3), that the combined integrals over the surfaces λ_a and λ_b vanish. The perturbation velocity potential can, therefore, be given alternatively as

$$\begin{aligned}\varphi(x,y,z)=&-\frac{1}{2\pi}\frac{\partial}{\partial x}\iint_{\tau}\left(\bar{\omega}\frac{\partial\varphi}{\partial n}-\varphi\frac{\partial\bar{\omega}}{\partial n}\right)d\bar{\Sigma}+\\&\frac{k}{2\pi}\frac{\partial}{\partial x}\iiint_{\bar{V}}\frac{1}{2}\varphi_{x_1}^2\left(\frac{\partial\bar{\omega}}{\partial x_1}\right)d\bar{V}\end{aligned} \tag{29}$$

Equations (27) and (29) may now be written in the various forms

$$\varphi(x,y,z)=\varphi_L(x,y,z)+\frac{k}{2\pi}\frac{\partial}{\partial x}\iiint_{\bar{V}}\frac{1}{2}\varphi_{x_1}^2\left(\frac{\partial\bar{\omega}}{\partial x_1}\right)d\bar{V} \tag{30a}$$

$$=\varphi_L(x,y,z)-\frac{k}{2\pi}\frac{\partial}{\partial x}\iiint_{\bar{V}}\frac{1}{2}\varphi_{x_1}^2\frac{1}{\bar{\sigma}}d\bar{V} \tag{30b}$$

$$\begin{aligned}=\varphi_L(x,y,z)&-\frac{1}{2\pi}\frac{\partial}{\partial x}\iint_{\lambda}\Delta\left(\frac{\partial\varphi}{\partial\bar{\nu}}\right)\bar{\omega}d\Sigma-\\&\frac{k}{2\pi}\frac{\partial}{\partial x}\iiint_{\bar{V}}\left(\frac{\partial}{\partial x_1}\frac{\varphi_{x_1}^2}{2}\right)\bar{\omega}\,d\bar{V}\end{aligned} \tag{30c}$$

$$\begin{aligned}=\varphi_L(x,y,z)&-\frac{1}{2\pi}\iint_{\lambda}\Delta\left(\frac{\partial\varphi}{\partial\bar{\nu}}\right)\frac{1}{\bar{\sigma}}d\bar{\Sigma}-\\&\frac{k}{2\pi}\iiint_{\bar{V}}\left(\frac{\partial}{\partial x_1}\frac{\varphi_{x_1}^2}{2}\right)\frac{1}{\bar{\sigma}}d\bar{V}\end{aligned} \tag{30d}$$

where φ_L has the same analytic form as in linearized supersonic theory and use has been made of the relations

$$\left.\begin{aligned}\bar{\omega}&=\cosh^{-1}\frac{x-x_1}{\beta[(y-y_1)^2+(z-z_1)^2]^{1/2}}\\\frac{\partial\bar{\omega}}{\partial x_1}&=\frac{-1}{[(x-x_1)^2-\beta^2(y-y_1)^2-\beta^2(z-z_1)^2]^{1/2}}=-\frac{1}{\bar{\sigma}}\end{aligned}\right\} \tag{31}$$

Comparison of equations (23) and (30) shows once more a difficulty that appears in linearized analysis of subsonic and supersonic flow, namely, that complete parallelism between the formulas is not achieved directly. This parallelism can only be established after interchanging the order of integration and differentiation and, because of the singularities involved, it becomes necessary to introduce the concept of finite-part integration. Furthermore, it is well known that the resulting multiple integrals can no longer be written in a unique form (see, e. g., ref. 25) but must be expressed differently, depending on the order in which the integrations are to be performed. No attempt will be made to develop these ideas further at the present time.

CALCULATION OF CONDITIONS ON SHOCK SURFACES

It is of some interest to study equations (23a), (23b), (30a), and (30b) as the field point approaches a discontinuity surface and to discover the mechanism by means of which these basic equations furnish the velocity jumps associated with the shock waves in the field. To this end, consider first the case $M_\infty \geqq 1$. Figure 4 shows the geometry of the problem. The bow wave induced by an aerodynamic shape is indicated

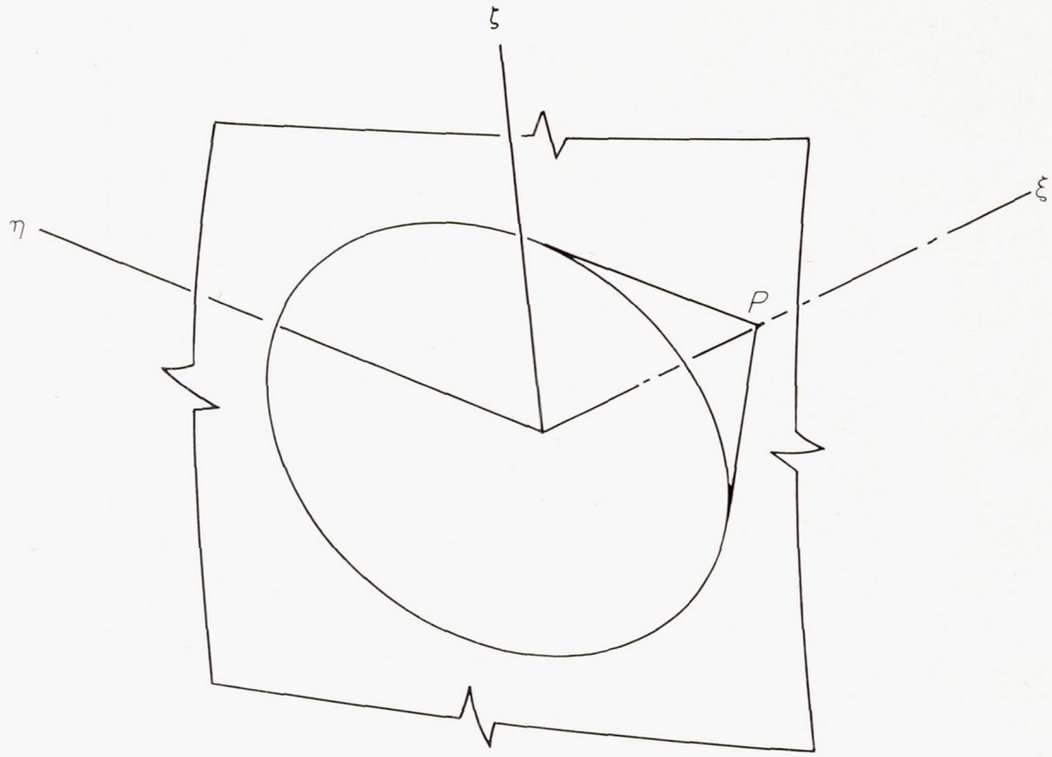

FIGURE 4.—View of element of shock wave and coordinate system.

and the point P, at which conditions are to be calculated, is chosen arbitrarily close to the rear surface of the wave. The surface of the wave can be replaced locally by a planar element and a new coordinate system ξ, η, ζ introduced with the origin fixed at the intersection of the line $y_1=y$, $z_1=z$, and the bow wave. Point P then has the coordinates ξ, 0, 0 and the planar surface is given by the linear relation

$$a\xi_1+b\eta_1+c\zeta_1=0 \tag{32}$$

Since the bow wave is situated upstream of the linearized disturbance field, u_L is zero and, from equation (30a), the perturbation velocity is

$$u(\xi,0,0)=\frac{k}{2\pi}\frac{\partial^2}{\partial\xi^2}\iiint\frac{u^2}{2}\left(\frac{\partial\overline{\omega}}{\partial\xi_1}\right)d\zeta_1 d\eta_1 d\xi_1 \tag{33}$$

where $\overline{\omega}=\cosh^{-1}[(\xi-\xi_1)/\beta(\eta_1^2+\zeta_1^2)^{1/2}]$. By virtue of the field point's nearness to the bow wave, the term $u^2/2$ in the integrand is assumed a constant and one then gets

$$u(\xi,0,0)=\frac{k}{2\pi}\frac{u^2}{2}\frac{\partial^2}{\partial\xi^2}\int_{Z_1}^{Z_2}d\zeta_1\int_{Y_1}^{Y_2}d\eta_1\int_{X_1}^{X_2}\frac{\partial\omega}{\partial\xi_1}d\xi_1$$

where

$$X_1=-(b\eta_1+c\zeta_1)/a,\qquad X_2=\xi-\beta(\eta_1^2+\zeta_1^2)^{1/2}$$

$$Y_1,Y_2=\frac{b(a\xi+c\zeta_1)\pm a\beta[a^2\xi^2+2ac\xi\zeta_1-(a^2\beta^2-b^2-c^2)\zeta_1^2]^{1/2}}{a^2\beta^2-b^2}$$

$$Z_1,Z_2=\frac{a\xi[c\pm(a^2\beta^2-b^2)^{1/2}]}{a^2\beta^2-b^2-c^2}$$

Integration and differentiation yields

$$u(\xi,0,0)=\frac{ku^2}{2}\frac{a^2}{-a^2\beta^2+b^2+c^2} \tag{34}$$

It remains to show that this result, derived from the integral expression for the perturbation velocity potential, is consistent with the result one would get from the shock-polar relation of equation (3). At the downstream face of the bow wave, equation (3) becomes

$$-\beta^2u_b^2+v_b^2+w_b^2=ku_b^3/2$$

The incremental velocity vector occurring at the shock surface is, however, normal to the shock surface and this yields the relations $u_b:v_b:w_b=a:b:c$. Substitution into the shock polar relation gives

$$u_b=-\frac{ku_b^2}{2}\left(\frac{u_b^2}{\beta^2u_b^2-v_b^2-w_b^2}\right)=\frac{ku_b^2}{2}\frac{a^2}{-a^2\beta^2+b^2+c^2} \tag{35}$$

in agreement with equation (34). It therefore follows that the integral expression, for $M_\infty\geqq 1$, will adapt itself on the shock surface to any bow wave consistent with given body geometry. This result can also be extended to include any shock wave in the flow field.

An analogous procedure follows for the case $M_\infty\leqq 1$. Let the shock surface in the vicinity of the point P at ξ,0,0 be given by equation (32) and assume that u^2 is composed of a continuous part and a discontinuous part that has the constant value u_a^2 ahead of and u_b^2 behind the shock. Equation (23a) then yields

$$\lim_{\xi\to 0}[u(\xi-,0,0)-u(\xi+,0,0)]=$$
$$\lim_{\xi\to 0}\frac{k}{4\pi}(u_a^2-u_b^2)\frac{\partial}{\partial\xi}\iint\frac{a\,d\zeta_1 d\eta_1}{[(a\xi+b\eta_1+c\zeta_1)^2+a^2\beta^2\eta_1^2+a^2\beta^2\zeta_1^2]^{1/2}} \tag{36}$$

where the double integration extends over the region of

discontinuity. If the differentiation with respect to ξ is now carried within the integral signs and ξ allowed to approach zero, the value of the integral becomes independent of the original limits of integration. In this way one gets

$$u_a-u_b=\lim_{\xi\to 0}\,[u(\xi-,0,0)-u(\xi+,0,0)]=\frac{ka^2}{a^2\beta^2+b^2+c^2}\,\frac{u_a^2-u_b^2}{2} \tag{37}$$

It can be shown, as previously, that equation (37) agrees with the result given by equation (3), the shock polar condition, for $M_\infty \leqq 1$.

REDUCTION TO SONIC FLOW THEORY

In this section, the previously determined equations will be studied in the limit as sonic, free-stream speed is reached. The integral relations then assume forms that correspond to the nonlinear differential equation when $\beta=0$.

INTEGRATED STRENGTHS OF EXTERNAL SOURCES

It is proposed here to determine a relation that will prove useful in the following section in connection with the reduction of the integral equations to the special forms appropriate for $M_\infty=1$. This relation will be recognized subsequently as connecting the integrated strengths of the exterior corrective sources in the crossplane $x=x_o=$const. and the rate of change of body cross-section area. As a means to this end, equation (10) is written in the form

$$k\,\frac{\partial}{\partial x}\,\frac{u^2(x,y,z)}{2}=\beta^2\,\frac{\partial u(x,y,z)}{\partial x}+\nabla^2\varphi \tag{38}$$

where ∇^2 is the two-dimensional Laplacian operator in the transverse plane. Each term is then integrated over the entire $x=x_o$ plane external to the body. The double integral involving $\nabla^2\varphi$ can be partially integrated and converted into a line integral by application of Green's theorem for a plane

$$\iint(\nabla^2\varphi)_{x=x_o}dydz=-\int_C\left(\frac{\partial\varphi}{\partial n}\right)_{x=x_o}d\sigma_c \tag{39}$$

where the line or curvilinear integral extends around the curves C enclosing the region of integration of the double integral. For cases in which the plane $x=x_o$ does not intersect any shock waves, the region of integration can be taken at once as the entire $x=x_o$ plane exterior to the body. If the assumption is made, as in linear subsonic theory, that the normal gradient of φ attenuates with lateral distance sufficiently fast to suppress the contribution of the curvilinear integral along the outer boundary, the boundary conditions of equation (8) permit one to equate the line integral along C to $-U_\infty S'(x_o)$ where $S'(x_o)$ denotes the longitudinal gradient of body cross-section area. The integrated form of equation (38) thus becomes

$$k\iint\left(\frac{\partial}{\partial x}\,\frac{u^2}{2}\right)_{x=x_o}dydz=\beta^2\iint\left(\frac{\partial u}{\partial x}\right)_{x=x_o}dydz-U_\infty S'(x_o) \tag{40}$$

In the more general case, however, in which the plane $x=x_o$ intersects a shock wave as illustrated in figure 5, discontinuities occur which require that the integration region must be divided into two parts, one lying between the body and the shock wave and the other extending beyond the shock wave to infinity. Application of Green's theorem to each region and addition of the separate contributions results in additional line integrals carried around the two sides of the shock surface. These two line integrals can be combined into a single line integral, in which case equation (40) can be written as follows

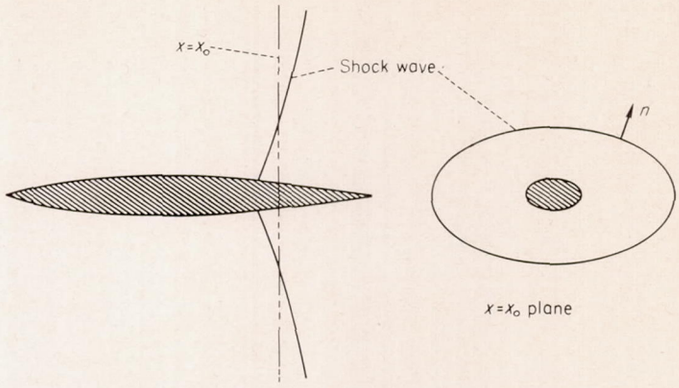

FIGURE 5.—View illustrating intersection of shock wave and $x=x_o$ plane.

$$k\iint\left(\frac{\partial}{\partial x}\,\frac{u^2}{2}\right)_{x=x_o}dydz+\int_\lambda\left[\Delta\left(\frac{\partial\varphi}{\partial n}\right)\right]_{x=x_o}d\sigma_\lambda=$$
$$\beta^2\iint\left(\frac{\partial u}{\partial x}\right)_{x=x_o}dydz-U_\infty S'(x_o) \tag{41}$$

where $\Delta(\partial\varphi/\partial n)=\partial\varphi_a/\partial n-\partial\varphi_b/\partial n$ and where in the single line integral the integration extends around the curve described by the intersection of the shock wave and the $x=x_o$ plane, and the normal n is taken as directed away from the body.

In the subsequent work, attention is to be directed toward results at $M_\infty=1$. We assume here that in the limit as $\beta\to 0$ the first term in the right-hand member of equation (41) will vanish and one then gets

$$k\iint\left(\frac{\partial}{\partial x}\,\frac{u^2}{2}\right)_{x=x_o}dy\,dz+\int_\lambda\left(\Delta\,\frac{\partial\varphi}{\partial n}\right)_{x=x_o}d\sigma_\lambda=-U_\infty S'(x_o) \tag{42}$$

It will become evident in the discussion contained in the following section that the left side of equation (42) represents the integrated strengths of the exterior corrective sources in the cross-plane $x=x_o=$const. in the limit as M_∞ approaches 1. It follows that under conditions corresponding to sonic flight speed, the total source strength in any transverse plane is zero: The sum of the sources within the body or wing (sources appearing in the term φ_L) is of equal magnitude but opposite sign to the corrective sources required by the nonlinear term in the differential equation.

Equation (42) allows one to make some conclusions about the lateral attenuation of the x-wise gradient of u^2. Consider the double integral as written in terms of polar coordinates

$$k\iint\frac{\partial}{\partial x}\,\frac{u^2}{2}\,r_1dr_1d\theta_1$$

Since the definite integral must converge, it follows that the integrand attenuates faster than $1/r_1^2$ and if the assumption is made that the integrand has a purely algebraic character, one concludes that for large r_1

$$\frac{\partial}{\partial x}\frac{u^2}{2}\sim\frac{1}{r_1^{2+N}} \tag{43}$$

where N is some positive constant.

A check on equation (43) is provided by the work of Guderley and Yoshihara (ref. 26) on axially symmetric flow at sonic speed. In that analysis, for large r_1,

$$\frac{\partial}{\partial x}\frac{u^2}{2}\sim\frac{1}{r_1^{16/7}}$$

and this is in agreement with equation (43) when $N=2/7$. The same reference also gives

$$\frac{\partial\varphi}{\partial r_1}\sim\frac{1}{r_1^{9/7}}$$

which serves to substantiate the assumption made earlier that the curvilinear integral along the outer boundary can be neglected in equation (40).

INTEGRAL EQUATION FOR SLENDER BODIES, $M_\infty=1$

In the reduction of the integral equations to the case $\beta=0$, methods analogous to those employed in references 25 and 27 will be used. Attention will be confined here to field points at a finite distance from the body so that in the limit as β approaches zero, the term βr can be assumed to approach zero uniformly. As in conventional slender-body theory for linearized flow, the longitudinal distribution of cross-section area $S(x)$ is assumed to possess a continuous x-wise derivative. The method of reduction can be exhibited in a sufficiently general form if a lifting body of revolution is considered. When $M_\infty\leqq 1$, the perturbation potential for a body of revolution φ_B follows from equations (23) and for the purposes at hand the form (23d) is preferable. For sufficiently slender and smooth bodies the term φ_L can be expressed in terms of a rectilinear source and doublet distribution and the corrective source distribution appearing in the triple integral then extends over all space external to the x axis. If $\kappa(x)$ is the x-wise distribution of doublet strength, equation (23d) becomes

$$\varphi_B(x,r,\theta)=-\frac{U_\infty}{4\pi}\int_0^l\frac{S'(x_1)dx_1}{[(x-x_1)^2+\beta^2r^2]^{1/2}}-\frac{\sin\theta}{4\pi r}\frac{\partial}{\partial x}\int_0^\infty\frac{(x-x_1)\kappa(x_1)dx_1}{[(x-x_1)^2+\beta^2r^2]^{1/2}}-\frac{1}{4\pi}\frac{\partial}{\partial x}\iint_\lambda\left(\Delta\frac{\partial\varphi}{\partial\nu}\right)_B\frac{(x-x_1)}{|x-x_1|}\,ln\,\frac{|x-x_1|+[(x-x_1)^2+\beta^2\rho_{II}^2]^{1/2}}{\beta\rho_{II}}d\Sigma-$$

$$\frac{k}{4\pi}\frac{\partial}{\partial x}\iiint_V\left(\frac{\partial}{\partial x_1}\frac{\varphi_{x_1}^2}{2}\right)_B\frac{(x-x_1)}{|x-x_1|}\,ln\,\frac{|x-x_1|+[(x-x_1)^2+\beta^2\rho_{II}^2]^{1/2}}{\beta\rho_{II}}r_1dr_1dx_1d\theta_1 \tag{44}$$

In equation (44), cylindrical coordinates x, r, θ are used where $r^2=y^2+z^2$, $\theta=\tan^{-1}(z/y)$ and the notation

$$\rho_{II}=[r^2+r_1^2-2rr_1\cos(\theta-\theta_1)]^{1/2}$$

has been introduced.

Under the imposed conditions, the first two terms in the right member of equation (44) reduce, as shown for example in reference 27, to approximately

$$\frac{U_\infty}{2\varphi}S'(x)\,ln\,r-\frac{\kappa(x)\sin\theta}{2\pi r}-\frac{U_\infty}{4\pi}\frac{\partial}{\partial x}\int_0^l S'(x_1)\frac{x-x_1}{|x-x_1|}\,ln\,\frac{2|x-x_1|}{\beta}dx_1$$

It remains to attempt a corresponding modification of the two remaining integrals. Consider, next, the triple integral. Since the integration extends over all points in space, one encounters a nonuniformity of convergence in the logarithmic influence function when β becomes vanishingly small and r_1 becomes infinitely large. From equation (43), however, it is known that $\partial u^2/\partial x$ attenuates rapidly with increasing r_1 and the resultant error in miscalculating the effect of the logarithm for large r_1 is thereby reduced. The triple integral is therefore approximated by

$$-\frac{k}{2\pi}\frac{\partial}{\partial x}\iiint_V\left[\frac{\partial}{\partial x_1}\frac{u_B^2(x_1,r_1,\theta_1)}{2}\right]\frac{x-x_1}{|x-x_1|}\,ln\,\frac{2|x-x_1|}{\beta\rho_{II}}dx_1r_1dr_1d\theta_1$$

This term can be rewritten as

$$\frac{k}{2\pi}\iint\left[\frac{\partial}{\partial x}\frac{u_B^2(x,r_1,\theta_1)}{2}\right]ln\,\rho_{II}r_1dr_1d\theta_1-$$

$$\frac{k}{4\pi}\frac{\partial}{\partial x}\int\frac{x-x_1}{|x-x_1|}\,ln\,\frac{2|x-x_1|}{\beta}dx_1\iint\left[\frac{\partial}{\partial x_1}\frac{u_B^2(x_1,r_1,\theta_1)}{2}\right]r_1dr_1d\theta_1$$

Consider, finally, the integral over the shock surface. For β near zero, one gets the expression

$$-\frac{1}{4\pi}\frac{\partial}{\partial x}\iint_\lambda\left(n_2\Delta\frac{\partial\varphi_B}{\partial y}+n_3\Delta\frac{\partial\varphi_B}{\partial z}\right)\frac{x-x_1}{|x-x_1|}\,ln\,\frac{2|x-x_1|}{\beta\rho_{II}}d\Sigma$$

which becomes

$$\frac{1}{2\pi}\int_\lambda\Delta\frac{\partial\varphi_B}{\partial n}(x,y_1,z_1)ln\,\rho_{II}d\sigma_\lambda-$$

$$\frac{1}{4\pi}\frac{\partial}{\partial x}\int\frac{x-x_1}{|x-x_1|}\,ln|x-x_1|dx_1\int\Delta\frac{\partial\varphi_B}{\partial n}(x,y_1,z_1)d\sigma_\lambda$$

where $d\sigma_\lambda$ represents an element of arc on the curve determined by the intersection of the shock surface and a plane normal to the x axis. The normal n, as in equation (42), is directed away from the body.

The reduced form of equation (44), for the case $M_\infty=1$, is given by the sum of the above three expressions. In the forms given, an apparent dependence on β remains in the expression

$$-\frac{1}{4\pi}\frac{\partial}{\partial x}\int\frac{x-x_1}{|x-x_1|}\,ln\,\frac{2|x-x_1|}{\beta}dx_1\left[U_\infty S'(x_1)+\right.$$

$$\left.k\iint\frac{\partial}{\partial x_1}\frac{u_B^2(x_1,r_1,\theta_1)}{2}r_1dr_1d\theta_1+\int_\lambda\Delta\frac{\partial\varphi_B}{\partial n}(x,y_1,z_1)d\sigma_\lambda\right]$$

The bracketed term vanishes by virtue of equation (42), however, and the dependence on β disappears. The sonic form of the integral equation for the lifting body of revolution is, therefore,

$$\varphi_B(x,r,\theta)=\frac{U_\infty S'(x)}{2\pi}\,lnr-\frac{\kappa(x)\sin\theta}{2\pi r}+\frac{1}{2\pi}\int_\lambda \Delta\frac{\partial\varphi_B}{\partial n}\,ln\rho_{\rm II}d\sigma_\lambda+\frac{k}{2\pi}\iint\left(\frac{\partial}{\partial x}\frac{u_B^2}{2}\right)ln\rho_{\rm II}r_1dr_1d\theta_1 \quad (45)$$

Starting under the assumption that $M_\infty \geqq 1$ and using equation (30d), one can derive the same result, the only essential difference arising from the fact that in the limiting process care must be taken to restrict the disturbance region $\overline{V}$ to that portion of space within the Mach forecone from the field point at x,y,z.

Equation (45) expresses the sonic equation in the form

$$\varphi_B(x,r,\theta)=\varphi_{2_B}(x;r,\theta)+\frac{1}{2\pi}\int_\lambda \Delta\frac{\partial\varphi_B}{\partial n}\,ln\rho_{\rm II}d\sigma_\lambda+\frac{k}{2\pi}\iint\left(\frac{\partial}{\partial x}\frac{u_B^2}{2}\right)ln\rho_{\rm II}r_1dr_1d\theta_1 \quad (46)$$

where $\varphi_{2_B}(x;r,\theta)$ is the harmonic potential for the body of revolution in transverse planes. As expressed, this sonic form of the integral equation for the perturbation potential is identical to the integral equation corresponding to the transonic differential equation at $\beta=0$; that is, it gives, for a flow field in which shock waves may possibly occur, the integral equation corresponding to the partial differential equation

$$\varphi_{yy}+\varphi_{zz}=\frac{\gamma+1}{U_\infty}\varphi_x\varphi_{xx} \quad (47a)$$

and admits discontinuity surfaces for which the difference relation

$$(\varphi_{y_a}-\varphi_{y_b})^2+(\varphi_{z_a}-\varphi_{z_b})^2=\frac{\gamma+1}{U_\infty}\frac{\varphi_{x_a}+\varphi_{x_b}}{2}(\varphi_{x_a}-\varphi_{x_b})^2 \quad (47b)$$

is satisfied. The direct derivation of equation (46) would follow from an application of Green's theorem in the transverse variables to equation (47a) without the introduction of the slender-body assumptions.

The interpretation of equation (42) in terms of net source strengths is now apparent. Each of the three terms in the right member of equation (46) provides two-dimensional sources in each transverse plane x_1=const. and the perturbation flow field is simulated by the combined effect of these sources and in lifting cases, a doublet term. (The doublet term is of no concern in the present discussion since its net source strength is zero.) The first term, φ_{2_B}, contains a source on the x axis with strength fixed by the gradient of area, $S'(x)$; the second term represents a curvilinear distribution of sources around the shock wave with strengths fixed by $\Delta(\partial\varphi/\partial n)$; the last term represents a planar distribution of sources with strengths determined by the nonlinear term $(k/2)(\partial/\partial x)\varphi_x^2$. Equation (42) thus states that at $M_\infty=1$ the combined source strength must vanish in each transverse plane.

Equation (46) corresponds, for the body of revolution at $M_\infty=1$, to equations (23c) and (30d) in that it contains an explicit contribution from the shock wave and is expressed in terms of the basic singularities of the differential equation. A form analogous to equations (23b) and (30b) can also be derived as follows. Let $r=R(x,\theta)$ be the equation of the shock surface. The relation

$$\frac{k}{2\pi}\frac{\partial}{\partial x}\int_o^{2\pi}d\theta_1\int_o^\infty\frac{u_B^2}{2}\,ln\rho_{\rm II}r_1dr_1d\theta_1=\frac{k}{2\pi}\frac{\partial}{\partial x}\int_o^{2\pi}d\theta_1\left[\int_0^{R(x,\theta_1)}+\int_{R(x,\theta_1)}^\infty\right]\frac{u_B^2}{2}\,ln\rho_{\rm II}r_1dr_1=\frac{k}{2\pi}\int_o^{2\pi}d\theta_1\int_o^\infty\frac{\partial}{\partial x}\frac{u_B^2}{2}\,ln\rho_{\rm II}r_1dr_1d\theta_1-\frac{k}{2\pi}\int_o^{2\pi}R(x,\theta_1)\frac{\partial R(x,\theta_1)}{\partial x}\left(\Delta\frac{u_B^2}{2}\,ln\rho_{\rm II}\right)_{r_1=R(x,\theta_1)}d\theta_1$$

then holds. Substitution into equation (46) yields

$$\varphi_B(x,r,\theta)=\varphi_{2_B}(x;r,\theta)+\frac{1}{2\pi}\int_\lambda\Delta\left\{\frac{\partial\varphi_B}{\partial n}-\frac{\frac{\partial R}{\partial x}\frac{k}{2}u_B^2}{\left[1+\left(\frac{1}{R}\frac{\partial R}{\partial\theta}\right)^2\right]^{1/2}}\right\}ln\rho_{\rm II}d\sigma_\lambda+\frac{k}{2\pi}\iint\frac{u_B^2}{2}ln\rho_{\rm II}r_1dr_1d\theta_1$$

and through use of equation (47b) one gets

$$\varphi_B(x,r,\theta)=\varphi_{2_B}(x;r,\theta)+\frac{k}{2\pi}\frac{\partial}{\partial x}\iint\frac{u_B^2}{2}\,ln\rho_{\rm II}r_1dr_1d\theta_1 \quad (48)$$

The above results have been worked out in some detail for the body of revolution. The sonic equations for other shapes follow similarly through a reduction of the general transonic integral equations or can be expressed directly through consideration of the sonic differential equation. The final equations for both cases appear as follows:

$$\varphi(x;y,z)=\varphi_2(x;y,z)+\frac{k}{2\pi}\frac{\partial}{\partial x}\iint\frac{u_B^2}{2}\,ln\rho_{II}r_1dr_1d\theta_1 \quad (49a)$$

$$=\varphi_2(x;y,z)+\frac{1}{2\pi}\int_\lambda\Delta\frac{\partial\varphi_B}{\partial n}\,ln\rho_{II}d\sigma_\lambda+\frac{k}{2\pi}\iint\frac{\partial}{\partial x}\frac{u_B^2}{2}\,ln\rho_{II}r_1dr_1d\theta_1 \quad (49b)$$

where $\varphi_2(x;y,z)$ is a two-dimensional harmonic function which, for the body of revolution and for the planar wing is, respectively,

$$\varphi_{2_B}=\frac{U_\infty S'(x)}{2\pi}\,ln\,r-\frac{\kappa(x)\sin\theta}{2\pi r} \tag{50a}$$

$$\varphi_{2_W}=\frac{1}{2\pi}\int_{-s_1(x)}^{s_2(x)}\Delta w_W(x;y_1)ln[(y-y_1)^2+z^2]^{1/2}dy_1+$$

$$\frac{1}{2\pi}\int_{-s_1(x)}^{s_2(x)}\Delta\varphi_W(x;y_1)\frac{z\,dy_1}{[(y-y_1)^2+z^2]} \tag{50b}$$

In the latter expression,

$$\Delta w(x;y_1)=w(x;y_1)_{z=0+}-w(x;y_1)_{z=0-}$$

$$\Delta\varphi(x;y_1)=\varphi(x;y_1)_{z=0+}-\varphi(x;y_1)_{z=0-}$$

and the lateral boundaries of the wing plan form are fixed by $-s_1(x)$ and $s_2(x)$.

SLENDER-WING THEORY IN LINEARIZED FLOW

In the preceding development, the integral realation for the perturbation potential in sonic flow has been expressed in a form that follows from an application to equation (47a) of Green's theorem in transverse planes. The determination of a solution thus depends to a large extent on the evaluation of the effect of the two-dimensional singularities that are placed throughout the exterior portion of the flow field. Examples of a direct attack on a similar problem are to be found in the calculations of two-dimensional transonic flows by Oswatitsch, Gullstrand, and Spreiter and Alksne, references 9 through 15. In the present report, an indirect attack is to be made, following the ideas of Whitcomb and Oswatitsch (refs. 6 and 7) by relating the solution for a slender wing to that of a body of revolution. The analysis will show that once one establishes the details of the crossflow potential fields associated with a wing and its related body of revolution, the residual disturbance fields near the two bodies are the same to a certain order of accuracy in terms of the slenderness ratio. The mechanics of such an approach can, in fact, be observed in linearized wing theory and such a development will be given in this section as a prelude to the subsequent sonic theory. Attention will be limited to the subsonic case and, as an added simplification in the analysis, only wings possessing lateral symmetry will be considered although such a restriction is not essential.

ANALYSIS

The linearized equation for subsonic potential flow is

$$\varphi_{yy}+\varphi_{zz}=-\beta^2\varphi_{xx} \tag{51}$$

and if Green's theorem is applied, formal manipulation leads to the following integral relation for the potential φ_w of a planar wing

$$\varphi_W(x,y,z)=\varphi_{2_W}(x;y,z)-\frac{\beta^2}{2\pi}\iint\varphi_{xx_W}(x,r_1,\theta_1)ln[r^2+r_1^2-$$

$$2rr_1\cos(\theta-\theta_1)]^{1/2}r_1dr_1d\theta_1 \tag{52}$$

No integrals along possible discontinuity surfaces are necessary since shock waves do not appear in linearized subsonic flow theory. Equation (52) is linear in φ and can be separated into additive expressions contributing to $\varphi_{W,t}$, the potential associated with the thickness distribution, and $\varphi_{W,\alpha}$, the potential associated with camber and angle of attack. In this way one gets for the perturbation velocity components

$$u_{W,t}=u_{2_{W,t}}-\frac{\beta^2}{2\pi}\frac{\partial}{\partial x}\iint\varphi_{xx_{W,t}}ln[r^2+r_1^2-2rr_1\cos(\theta-\theta_1)]^{1/2}r_1dr_1d\theta_1 \tag{53a}$$

$$w_{W,t}=w_{2_{W,t}}-\frac{\beta^2}{2\pi}\frac{\partial}{\partial x}\iint\varphi_{xx_{W,t}}ln[r^2+r_1^2-2rr_1\cos(\theta-\theta_1)]^{1/2}r_1dr_1d\theta_1 \tag{53b}$$

and

$$u_{W,\alpha}=u_{2_{W,\alpha}}-\frac{\beta^2}{2\pi}\frac{\partial}{\partial x}\iint\varphi_{xx_{W,\alpha}}ln[r^2+r_1^2-2rr_1\cos(\theta-\theta_1)]^{1/2}r_1dr_1d\theta_1 \tag{54a}$$

$$w_{W,\alpha}=w_{2_{W,\alpha}}-\frac{\beta^2}{2\pi}\frac{\partial}{\partial z}\iint\varphi_{xx_{W,\alpha}}ln[r^2+r_1^2-2rr_1\cos(\theta-\theta_1)]^{1/2}r_1dr_1d\theta_1 \tag{54b}$$

The corrective integrals in equations (53) and (54) obviously do not modify the area distribution in the thickness case by virtue of the vertical symmetry in the flow field nor the load distribution in the camber case by virtue of the vertical asymmetry in the field. It follows that

$$\Delta w_{W,t}=\Delta w_{2_{W,t}},\qquad \Delta u_{W,\alpha}=\Delta u_{2_{W,\alpha}} \tag{55}$$

where the delta notation denotes the increment in the function in passing through the plane $z=0$, that is, the difference between the values on the upper and lower surfaces of the wing. As a consequence, φ_{2_W} can be expressed in the form

$$\frac{\varphi_{2_W}(x;y,z)}{U_\infty}=\frac{1}{2\pi}\int_{-s(x)}^{s(x)}\frac{\Delta w_{W,t}}{U_\infty}ln(r^2+y_1^2-2ry_1\cos\theta)^{1/2}dy_1+$$

$$\frac{1}{2\pi}\int_{-s(x)}^{s(x)}\frac{\Delta\varphi_{W,\alpha}}{U_\infty}\frac{r\sin\theta dy_1}{r^2+y_1^2-2ry_1\cos\theta} \tag{56}$$

If exact conditions on the wing surface are to be sought in linearized theory, equations (53a) must also be satisfied. For example, in the direct case of given thickness, equation (56) predicts $u_{2_{W,t}}$ and equation (53b) is then used to determine the exact streamwise velocity component as affected by the external-source integral. In the direct case of given loading, equation (56) predicts $w_{2_{W,\alpha}}$ and equation (54b) is then used to calculate the true wing camber, modification of $w_{2_{W,\alpha}}$ being produced by the integral term. The difficulties of such calculations are so disproportionate to those of solving the linearized equation by standard methods that they appear to add needless complications to a relatively simple problem. In transonic theory, however, the right-hand member of equation (51) is replaced by a nonlinear term and, in the absence of more obvious methods of attack, the difficulties involved in such an approach become less of a deterrent; in particular, the integral forms of the corrective terms are of added interest since they are suited to approximations. The details of such an approach will not be considered further

at the present time since for slender wings the use of a related body of revolution yields information of a sufficient order of exactness in both linear and nonlinear theory.

In the following work, a complete knowledge of the solution for a body of revolution will be assumed known. Thus, if $S(x)$ is the cross-sectional area of the body and the distribution of lift is fixed by $\kappa(x)$, doublet strength per unit of length, the linearized solution for the body of revolution is

$$\frac{\varphi_B(x,r,\theta)}{U_\infty}=-\frac{1}{4\pi}\int_0^l \frac{S'(x_1)dx_1}{[(x-x_1)^2+\beta^2r^2]^{1/2}}-\frac{\beta^2 r\sin\theta}{4\pi}\int_0^\infty \frac{\kappa(x_1)dx_1}{[(x-x_1)^2+\beta^2r^2]^{3/2}} \tag{57}$$

and the perturbation potential in the transverse plane is

$$\frac{\varphi_{2_B}(x;r,\theta)}{U_\infty}=\frac{S'(x)ln\,r}{2\pi}-\frac{\kappa(x)\sin\theta}{2\pi r} \tag{58}$$

The integral relations for the wing and the body combine to give

$$\varphi_W-\varphi_B=\varphi_{2_W}-\varphi_{2_B}-\frac{\beta^2}{2\pi}\iint(\varphi_W-\varphi_B)_{xx}\,ln[r^2+r_1^2-2rr_1\cos(\theta-\theta_1)]^{1/2}r_1\,dr_1\,d\theta_1 \tag{59}$$

Equation (59) is exact, subject only to the restrictions of first-order perturbation theory, but with added restrictions on the geometry and loading it is possible to show that the magnitude of the final integral is negligible to a certain order of accuracy. We now assume the wing is slender, that is, $s(x)$ is small in comparison with over-all wing length. Let, furthermore, the wing and body be of equal length and have identical longitudinal distributions of cross-sectional area. This implies

$$S'(x)=\int_{-s(x)}^{s(x)}\frac{\Delta w_W(x,y_1)dy_1}{U_\infty} \tag{60}$$

and establishes the condition that the distribution of two-dimensional source strength in equation (58) is equal to the strengths integrated in the transverse plane of the sources appearing in equation (56). It will also be convenient to equate in the same manner the doublet strengths in those two equations and one is led to the relation

$$\kappa(x)=-\int_{-s(x)}^{s(x)}\frac{\Delta\varphi_{2_W}(x,y_1)dy_1}{U_\infty} \tag{61}$$

The first objective will be to show that for field points in the vicinity of the slender wing the first two terms in the right member of equation (59) differ from the left member by an amount that is of higher order in s/l. The evaluation of the error term can be performed by an iterative process in which the first step starts with the approximation

$$\varphi_W\approx\varphi_{2_W}-\varphi_{2_B}+\varphi_B \tag{62}$$

Before integration, the integrand in equation (59) will be written as the product of Fourier expansions of its terms. For the logarithmic term, one has

$$ln[r^2+r_1^2-2rr_1\cos(\theta-\theta_1)]^{1/2}=\begin{cases} lnr_1-\sum_{m=1}^{\infty}\left(\frac{r}{r_1}\right)^m\frac{\cos m(\theta-\theta_1)}{m}, & r\leqq r_1\\ lnr-\sum_{m=1}^{\infty}\left(\frac{r_1}{r}\right)^m\frac{\cos m(\theta-\theta_1)}{m}, & r_1\leqq r\end{cases} \tag{63}$$

and, similarly,

$$\frac{r\sin\theta}{r^2+y_1^2-2ry_1\cos\theta}=\begin{cases}\frac{1}{y_1}\sum_{m=1}^{\infty}\left(\frac{y_1}{r}\right)^m\sin m\theta, & |y_1|\leqq r\\ \frac{1}{y_1}\sum_{m=1}^{\infty}\left(\frac{r}{y_1}\right)^m\sin m\theta, & r\leqq|y_1|\end{cases} \tag{64}$$

If equations (63) and (64) are used, together with equation (56), and conditions of bilateral symmetry are imposed, one gets

$$\frac{\varphi_{2W}(x;y,z)}{U_\infty l}=\frac{S'(x)}{2\pi l}lnr+\sum_{m=1}^{\infty}\frac{a_{2m}(x)\cos 2m\theta}{(r/s)^{2m}}+\sum_{m=1}^{\infty}\frac{b_{2m-1}(x)\sin(2m-1)\theta}{(r/s)^{2m-1}},\ s\leqq r \tag{65}$$

where

$$a_{2m}(x)=\frac{-s}{4\pi ml}\int_{-s(x)}^{s(x)}\frac{\Delta w_2(x,y_1)}{U_\infty}\left(\frac{y_1}{s}\right)^{2m}\frac{dy_1}{s} \tag{66a}$$

and

$$b_{2m-1}(x)=\frac{1}{2\pi l}\int_{-s(x)}^{s(x)}\frac{\Delta\varphi_2(x,y_1)}{U_\infty}\left(\frac{y_1}{s}\right)^{2m-2}\frac{dy_1}{s} \tag{66b}$$

Equation (65) holds true beyond the circle of radius $s(x)$ enclosing the transverse section of the wing; within this circle, the expression is

$$\frac{\varphi_{2W}(x;y,z)}{U_\infty l}=\frac{S'(x)}{2\pi l}lns+\sum_{n=0}^{\infty}\frac{A_{2n}(x)}{(2n+1)^2}\left[\left(\frac{r}{s}\right)^{2n+1}-1\right]+\sum_{m=1}^{\infty}\frac{\cos 2m\theta}{2m}\sum_{n=0}^{\infty}A_{2n}(x)\left[\left(\frac{r}{s}\right)^{2m}\frac{1}{2m-2n-1}-\left(\frac{r}{s}\right)^{2n+1}\left(\frac{1}{2m+2n+1}\right)+\left(\frac{1}{2m-2n-1}\right)\right]+\sum_{m=1}^{\infty}\sin(2m-1)\theta\sum_{n=0}^{\infty}B_{2n}(x)\left[\left(\frac{r}{s}\right)^{2m-1}\frac{1}{2n-2m+1}+\left(\frac{r}{s}\right)^{2n}\left(\frac{1}{2m+2n-1}+\frac{1}{2m-2n-1}\right)\right],\quad r\leqq s \tag{67}$$

where the coefficients A_{2n} and B_{2n} are related to the boundary conditions through the expansions

$$\frac{\Delta w_2(x,y_1)}{U_\infty}=\sum_{n=0}^{\infty}\frac{\pi lA_{2n}(x)}{s}\left(\frac{y_1}{s}\right)^{2n} \tag{68a}$$

$$\frac{\Delta\varphi_2(x,y_1)}{U_\infty l}=\sum_{n=0}^{\infty}\pi B_{2n}(x)\left(\frac{y_1}{s}\right)^{2n} \tag{68b}$$

Once the coefficients a_{2m}, b_{2m-1}, A_{2n}, and B_{2n} are related in magnitude to the geometry of the wing, the size of the integral term in equation (59) can be estimated. Since $\Delta w(x,y)/U_\infty$ is proportional to $t(x)/l$, the wing's thickness ratio, it follows from equations (66) and (68) that the following order estimates hold

$$a_{2m}(x)=0(ts/l^2),\qquad A_{2n}(x)=0(ts/l^2) \tag{69}$$

Let, furthermore, $\Delta\varphi(x,y)/U_\infty$ be assumed proportional to $\alpha(x)s(x)$ where $\alpha(x)$ is a measure of local angle of attack or camber; equations (66) and (68) then yield for the remaining coefficients

$$b_{2m-1}(x)=0(\alpha s/l), \qquad B_{2n}(x)=0(\alpha s/l) \tag{70}$$

Equation (67) can also be written in the simplified form

$$\frac{\varphi_{2W}(x;y,z)}{U_\infty l}=\frac{S'(x)}{2\pi l}\,lns+F\left(x,\frac{r}{s}\right)+\sum_{m=1}^{\infty}\frac{\cos 2m\theta}{2m}\,G_m\left(x,\frac{r}{s}\right)+\sum_{m=1}^{\infty}\sin(2m-1)\theta H_m\left(x,\frac{r}{s}\right), \qquad r\leqq s \tag{71}$$

with the order estimates

$$F\left(x,\frac{r}{s}\right)=0(ts/l^2), \qquad G_m\left(x,\frac{r}{s}\right)=0(ts/l^2), \qquad H_m\left(x,\frac{r}{s}\right)=0(\alpha s/l) \tag{72}$$

Evaluation of order of error in equation (62).—Equation (59) is now written in the form

$$\varphi_W(x,y,z)=\varphi_{2_W}(x;y,z)-\varphi_{2_B}(x;r,\theta)+\varphi_B(x,r,\theta)+I(x,r,\theta) \tag{73}$$

where

$$I(x,r,\theta)=-\frac{\beta^2}{2\pi}\int_0^\infty\int_0^{2\pi}\frac{\partial^2}{\partial x^2}(\varphi_W-\varphi_B)ln[r^2+r_1^2-2rr_1\cos(\theta-\theta_1)]^{1/2}r_1dr_1d\theta_1 \tag{74}$$

and an estimation of the order of magnitude of $I(x,r,\theta)$ is to be made for field points in the vicinity of the wing. The approximation of equation (62) is to be used together with the given expansions of the two-dimensional perturbation potentials. It suffices to simplify the analysis and estimate the order of the error at r equal to s. One then gets

$$\begin{aligned}\frac{I(x,s,\theta)}{U_\infty l}&\approx\frac{I_1(x,s,\theta)}{U_\infty l}+\frac{I_2(x,s,\theta)}{U_\infty l}\\
&=-\frac{\beta^2}{2\pi}\int_s^\infty\int_0^{2\pi}\left\{\sum_{m=1}^{\infty}\left[a''_{2m}(x)\left(\frac{s}{r_1}\right)^{2m}\cos 2m\theta_1+b''_{2m+1}(x)\left(\frac{s}{r_1}\right)^{2m+1}\sin(2m+1)\theta_1\right]\right\}\left[lnr_1-\sum_{n=1}^{\infty}\left(\frac{s}{r_1}\right)^n\frac{\cos n(\theta-\theta_1)}{n}\right]r_1dr_1d\theta_1-\\
&\quad\frac{\beta^2}{2\pi}\int_0^s\int_0^{2\pi}\left[\frac{S'''(x)}{2\pi l}\,ln\frac{s}{r_1}+F''\left(x,\frac{r_1}{s}\right)+\sum_{m=1}^{\infty}\frac{\cos 2m\theta_1}{2m}\,G''_m\left(x,\frac{r_1}{s}\right)+\sum_{m=1}^{\infty}\sin(2m-1)\theta_1H''_m\left(x,\frac{r_1}{s}\right)\right]\left[lns-\right.\\
&\quad\left.\sum_{n=1}^{\infty}\left(\frac{r_1}{s}\right)^n\frac{\cos n(\theta-\theta_1)}{n}\right]r_1dr_1d\theta_1\end{aligned} \tag{75}$$

After integration with respect to θ_1 one has

$$\begin{aligned}\frac{I(x,s,\theta)}{U_\infty l}&\approx\frac{\beta^2}{2}\int_s^\infty\sum_{m=1}^{\infty}\left[\frac{a''_{2m}(x)}{2m}\left(\frac{s}{r_1}\right)^{4m}\cos 2m\theta+\frac{b''_{2m+1}}{2m+1}\left(\frac{s}{r_1}\right)^{4m+2}\sin(2m+1)\theta\right]r_1dr_1-\beta^2\int_0^s\left[\frac{S'''(x)}{2\pi l}\,ln\frac{s}{r_1}+F''\left(x,\frac{r_1}{s}\right)\right]lnsr_1dr_1+\\
&\quad\frac{\beta^2}{2}\int_0^s\sum_{m=1}^{\infty}\left[\left(\frac{r_1}{s}\right)^{2m}\frac{\cos 2m\theta}{4m^2}\,G''_m\left(x,\frac{r_1}{s}\right)+\left(\frac{r_1}{s}\right)^{2m-1}\frac{\sin(2m-1)\theta}{(2m-1)^2}\,H''_m\left(x,\frac{r_1}{s}\right)\right]r_1dr_1\end{aligned}$$

From equations (69), (70), and (72), the order of magnitude of $I(x,s,\theta)/U_\infty l$ is given by

$$\frac{I(x,s,\theta)}{U_\infty l}\approx\beta^2 0\left(\frac{ts^3}{l^4}\,lns\right) \tag{76}$$

The first step in the iteration fixes the maximum value of the error incurred in neglecting the integral term of equation (74). In the vicinity of the wing, therefore, the perturbation potential can be expressed as in equation (62) with an error of the order given in equation (76).

Near the body, a further reduction of the difference $\varphi_B-\varphi_{2_B}$ is possible since the explicit equations for the body of revolution are available. This yields the usual form of the slender-wing solution. Thus, from equation (62),

$$\varphi_W\approx\varphi_{2_W}+f(x) \tag{77}$$

where

$$f(x)=\lim_{r\to 0}(\varphi_B-\varphi_{2_B})=-\frac{\beta^2}{2\pi}\int_0^{2\pi}\int_0^\infty\varphi_{xx_B}(x,r_1,\theta_1)lnr_1r_1dr_1d\theta_1 \tag{78}$$

From equation (57), $f(x)$ becomes, for the subsonic case,

$$\begin{aligned}f(x)&=-\frac{\beta^2U_\infty}{4\pi}\frac{\partial}{\partial x}\int_0^l(x-x_1)S'(x_1)dx_1\int_0^\infty\frac{lnr_1r_1dr_1}{[(x-x_1)^2+\beta^2r_1^2]^{3/2}}\\
&=-\frac{U_\infty}{8\pi}\frac{\partial}{\partial x}\int_0^l\frac{(x-x_1)}{|x-x_1|}S'(x_1)\left[ln\frac{(x-x_1)^2}{\beta^2}+ln4\right]dx_1\\
&=-\frac{U_\infty}{4\pi}\frac{\partial}{\partial x}\int_0^l\frac{(x-x_1)}{|x-x_1|}S'(x_1)ln\frac{2|x-x_1|}{\beta}dx_1\end{aligned} \tag{79a}$$

It is not difficult to show by a similar analysis taking into account the possibility of discontinuities in the flow that equation (77) holds also for $M_\infty>1$ and that $f(x)$ then has the form

$$f(x)=-\frac{U_\infty}{2\pi}\frac{\partial}{\partial x}\int_0^x S'(x_1)ln\frac{2(x-x_1)}{\beta}dx_1 \tag{79b}$$

SLENDER-WING THEORY IN SONIC FLOW

The extension of the foregoing derivation to the nonlinear case will be given in this section. The iteration procedure

designed to discuss the linear problem is effectively the development of an expansion in terms of the slenderness parameter of the wing and with appropriate restrictions on wing angle of attack can be applied with little modification.

ANALYSIS

Equation (49b), the relation fundamental to the following discussion, provides that the sonic expression for φ valid in the $x=x_0$ plane can be considered to be composed of three terms; φ_2, a line integral around the possible intersections of the $x=x_0$ plane and a shock wave, and a surface integral over the entire portion of the $x=x_0$ plane exterior to the body. In many important cases, simplification occurs because the line integral introduces no contribution to the values for φ in the vicinity of the body. Perhaps the simplest case in which this situation develops is that encountered very frequently at $M_\infty=1$ in which the shock waves are situated entirely downstream of the most rearward point. A second case in which the line integral introduces no contribution occurs when the discontinuity surface is situated in an $x=x_0$ plane and is, therefore, essentially a normal shock wave. The discontinuities associated with the normal shock wave are contained in the contribution of the double integral. Since most sonic flows about smooth wings or bodies probably fall into one of these two cases, attention will be confined in the following discussion to those cases in which no contribution results from the line integral. Thus, if equation (49b) is written first for a wing and then again for a body of revolution, and the latter is subtracted from the former, the following relation is obtained:

$$\varphi_W(x,y,z)=\varphi_{2_W}(x;y,z)-\varphi_{2_B}(x;r,\theta)+\varphi_B(x,r,\theta)+J(x,r,\theta) \tag{80}$$

where

$$J(x,r,\theta)=\frac{k}{2\pi}\int_0^\infty\int_0^{2\pi}\frac{1}{2}\frac{\partial}{\partial x}(u_W{}^2-u_B{}^2)\,ln\,[r^2-r_1{}^2-2rr_1\cos(\theta-\theta_1)]^{1/2}r_1,dr_1,d\theta_1 \tag{81}$$

The quadratic nature of the integrand in equation (81), together with the additive dependence on thickness and camber in the transverse-plane potentials, prompts one to simplify the analysis to cases involving a thin wing of given thickness but limited to an angle of attack or camber-length ratio α that is small in comparison with the thickness-length ratio t/l. In this way, sufficient information is retained to establish the relationship between the wing and body flow fields for the thickness case and at the same time determine a linear dependence on angle of attack of the wing loading in the vicinity of $\alpha=0$. Under these conditions it will be possible to relate the wing flow field to that of a body having the same area distribution but *not* inclined to the free stream. Consistent with these conditions, the following equations apply:

$$\varphi_{2_W}=\varphi_{2_{W,t}}+\varphi_{2_{W,\alpha}},\qquad \varphi_{2_B}=\varphi_{2_{B,t}} \tag{82}$$

and the perturbation potentials for the wing and body can be expressed as

$$\varphi_W=\varphi_{W,t}+\varphi_{W,\alpha},\qquad \varphi_B=\varphi_{B,t} \tag{83}$$

where the subscripts t and α identify the contributions attributable to thickness and camber. The term $u_W{}^2-u_B{}^2$ in the integrand of equation (81) can now be approximated by

$$u_W{}^2-u_B{}^2\approx(u_{2_{W,t}}-u_{2_{B,t}})^2+2u_{B,t}(u_{2_{W,t}}-u_{2_{B,t}})+(u_{2_{W,t}}-u_{2_{B,t}})u_{2_{W,\alpha}}+2u_{B,t}u_{2_{W,\alpha}} \tag{84}$$

where the initial assumption

$$\varphi_W\approx\varphi_{2_W}-\varphi_{2_{B,t}}+\varphi_{B,t} \tag{85}$$

has been made and higher order dependence on α has been deleted. It remains to show, through the evaluation of $J(x,r,\theta)$, that the assumption made in equation (85) holds. It should be noted that, to the order of exactness of this equation, normal shocks on the wing and body are situated at the same longitudinal station.

The first two terms in the right member of equation (84) depend solely on the thickness distribution of the wing and body, and the two remaining terms contain the effects attributable to the lift and thickness combined. Substituting from equation (84) into equation (81), we see that the first two terms contribute to $J(x,r,\theta)$ a function that is symmetric about $z=0$ and the two latter terms contribute an asymmetric quantity. From equation (80) one then gets

$$\Delta w_{W,t}=\Delta w_{2_{W,t}},\qquad \Delta u_{W,\alpha}=\Delta u_{2_{W,\alpha}}$$

These relations are identical to those given in equation (55) and, as a consequence, equation (56) necessarily remains valid along with the expansions given in equations (65) and (67).

We now approximate $J(x,r,\theta)$ at $r=s$:

$$\frac{J(x,s,\theta)}{U_\infty l}\approx\frac{J_1(x,s,\theta)}{U_\infty l}+\frac{J_2(x,s,\theta)}{U_\infty l}=\frac{k}{4\pi}\frac{\partial}{\partial x}\int_s^\infty\int_0^{2\pi}\left\{\left[\sum_{m=1}^\infty\frac{a'_{2m}(x)\cos 2m\theta_1}{(r_1/s)^{2m}}\right]^2+2u_{B,t}\sum_{m=1}^\infty\frac{a'_{2m}(x)\cos 2m\theta_1}{(r_1/s)^{2m}}+\left[\sum_{m=1}^\infty\frac{a'_{2m}(x)\cos 2m\theta_1}{(r_1/s)^{2m}}+2u_{B,t}\right]\sum_{\nu=1}^\infty\frac{b'_{2\nu-1}(x)\sin(2\nu-1)\theta_1}{(r_1/s)^{2\nu-1}}\right\}\left[ln r_1-\sum_{n=1}^\infty\left(\frac{s}{r_1}\right)^n\frac{\cos n(\theta-\theta_1)}{n}\right]r_1dr_1d\theta_1+\frac{k}{4\pi}\frac{\partial}{\partial x}\int_0^s\int_0^{2\pi}\left\{\left[\frac{S''(x)}{2\pi l}ln\frac{s}{r_1}+F'\left(x,\frac{r_1}{s}\right)+\sum_{m=1}^\infty\frac{\cos 2m\theta_1}{2m}G'_m\left(x,\frac{r_1}{s}\right)\right]^2+2u_{B,t}\left[\frac{S''(x)}{2\pi l}ln\frac{s}{r_1}+F'\left(x,\frac{r_1}{s}\right)+\sum_{m=1}^\infty\frac{\cos 2m\theta_1}{2m}G'_m\left(x,\frac{r_1}{s}\right)\right]+\left[\frac{S''(x)}{2\pi l}ln\frac{s}{r_1}+F'\left(x,\frac{r_1}{s}\right)+\sum_{m=1}^\infty\frac{\cos 2m\theta_1}{2m}G'_m\left(x_1\frac{r_1}{s}\right)+2u_{B,t}\right]\sum_{\nu=1}^\infty\sin(2\nu-1)\theta_1H'_\nu\left(x,\frac{r_1}{s}\right)\right\}\left[ln\,s-\sum_{n=1}^\infty\left(\frac{r_1}{s}\right)^n\frac{\cos n(\theta-\theta_1)}{n}\right]r_1dr_1d\theta_1 \tag{86}$$

The orthogonality of the trigonometric terms, together with the fact that $u_{B,t}$ has no dependence on θ, permits one to achieve considerable simplification after the θ_1 integration. The resulting expression is

$$\frac{J(x,s,\theta)}{U_\infty l}\approx\frac{k}{4\pi}\frac{\partial}{\partial x}\int_s^\infty\left\{\pi\sum_{m=1}^{\infty}\frac{a'_{2m}(x)^2}{(r_1/s)^{4m}}\,ln\,r_1-2\pi u_{B,t}\sum_{m=1}^{\infty}\left[\frac{\cos 2m\theta}{2m}\frac{a'_{2m}(x)}{(r_1/s)^{4m}}+\right.\right.$$

$$\left.\left.\frac{\sin(2m-1)\theta}{(2m-1)}\frac{b'_{2m-1}(x)}{(r_1/s)^{4m-2}}\right]+\cdots\right\}r_1dr_1+\frac{k}{4\pi}\frac{\partial}{\partial x}\int_0^s\int_0^{2\pi}\left[\frac{S''(x)}{2\pi l}\,ln\frac{s}{r_1}+F'\left(x,\frac{r_1}{s}\right)+\right.$$

$$\left.\sum_{m=1}^{\infty}\frac{\cos 2m\theta_1}{2m}G'_m\left(x,\frac{r_1}{s}\right)\right]^2 ln\,s\,r_1dr_1d\theta_1+\frac{k}{4\pi}\frac{\partial}{\partial x}\int_0^s 2\pi u_{B,t}\left\{2\left[\frac{S''(x)}{2\pi l}\,ln\frac{s}{r_1}+F'\left(x,\frac{r_1}{s}\right)\right]ln\,s-\right.$$

$$\left.\sum_{m=1}^{\infty}\frac{\cos 2m\theta}{4m^2}\left(\frac{r_1}{s}\right)^{2m}G'_m\left(x,\frac{r_1}{s}\right)-\sum_{m=1}^{\infty}\frac{\sin(2m-1)\theta}{(2m-1)}\left(\frac{r_1}{s}\right)^{2m-1}H'_m\left(x,\frac{r_1}{s}\right)\right\}r_1dr_1+\cdots$$

The convergence of all the terms in the first integral is assured when $u_{B,t}$ varies as $1/r^N$ for large r, N being any positive constant; for small r we assume $u_{B,t}$ varies directly with cross-sectional area of the body. The order of magnitude of $J(x,s,\theta)/U_\infty l$ can then be seen to be given by

$$\frac{J(x,s,\theta)}{U_\infty l}=0\left(\frac{t^2s^4}{l^6}\,ln\,s\right) \tag{87}$$

Since it follows from equations (85) and (56) that the magnitude of $\varphi_W/U_\infty l$ in the vicinity of the wing is $0[(ts/l^2)ln\ s]$, the relative error incurred by neglecting $J/U_\infty l$ is $0(ts^3/l^4)$.

Following the method used in deriving equation (77), we can achieve a final simplification in the wing's perturbation potential. Thus,

$$\varphi_W\approx\varphi_{2W}+g(x) \tag{88}$$

where

$$g(x)=\lim_{r\to 0}(\varphi_{B,t}-\varphi_{2_{B,t}})=k\int_0^\infty\frac{\partial}{\partial x}\frac{u_B{}^2(x,r_1)}{2}\,ln\,r_1\,r_1dr_1 \tag{89}$$

In the absence of analytical solutions for the body of revolution problem, the evaluation of $g(x)$ must be carried out by less direct methods. This will be discussed further in the section on applications.

APPLICATIONS TO SEVERAL PROBLEMS INVOLVING SONIC FLOW

In the following section, the exploitation of the results for sonic-flow conditions will be carried out in some detail. In view of the difficulty associated with transonic analysis, it appears likely that the equivalence relation of equation (85) will play an important part in the interpretation and use of experimental data as well as in purely theoretical predictions. The discussion will be concerned principally with applications to slender wings and bodies and to the relationships between the aerodynamic characteristics of the two configurations. It is obvious that the known basic information can be supplied either by theory or by experiment and many of the results to be given are written with the idea that they can be used in this dual sense.

RÉSUMÉ OF PRINCIPAL RESULTS OF SLENDER-BODY THEORY

It appears worthwhile, before proceeding to the examples, to re-examine the problem of transonic flow about slender bodies of arbitrary cross section from a heuristic, although less rigorous, point of view. This second approach may be regarded, if one prefers, as a physical interpretation of the result given in equation (80).

Consider the case of compressible flow about the slender body of arbitrary cross section shown in figure 6. The general procedure is to consider first the complete three-dimensional problem and then to introduce simplifying assumptions consistent with the restriction of slender plan forms. As in the more detailed analysis, it is again assumed that any shock waves are situated either entirely upstream of the most forward point of the body or entirely downstream of the most rearward point, or are normal shock waves if situated along the length of the body. The resulting solution for the perturbation potential can be expressed as the sum of four parts. As in the preceding analysis $\varphi_{2_{W,\alpha}}$, $\varphi_{2_{W,t}}$, and $\varphi_{2_{B,t}}$ are solutions of the two-dimensional Laplace equation as indicated. Thus $\varphi_{2_{W,\alpha}}$ corresponds to the two-dimensional incompressible-flow solution for translation of the cross section, and $\varphi_{2_{W,t}}$ to that for the growth of the cross section. In addition to satisfying the prescribed boundary conditions at the body surface, these two terms satisfy the requirement that the lateral velocity components $(\partial\varphi/\partial y,\ \partial\varphi/\partial z)$ vanish at infinity. These terms alone do not furnish a satisfactory approximation, however, for cases in which $S(x)$ is different from zero because $\varphi_{2_{W,t}}$ acts like $S'(x)\ ln\ r$ at large r, and

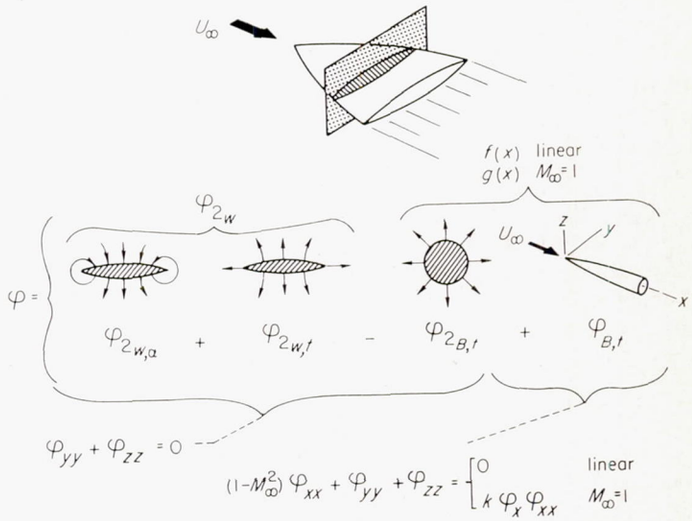

FIGURE 6.—Schematic representation of elements of slender-body theory.

hence $\partial\varphi/\partial x$ is infinite at a large lateral distance. This error can be removed, however, by subtracting the term $\varphi_{2_{B,t}}$ corresponding to the two-dimensional incompressible-flow solution for the growth of a body of revolution having the same $S(x)$ as the original body (thereby canceling $\varphi_{2_{W,t}}$ at large r), and adding the three-dimensional solution $\varphi_{B,t}$ for flow about the same body of revolution. If $\varphi_{B,t}$ is determined from linear theory, the results correspond to the familiar formulas of subsonic and supersonic slender-body theory. (This leads, in both cases, to the result given in equation (62) and reduces to equation (77) where, for subsonic flow, $f(x)$ has the form given in equation (79a) and, for supersonic flow, the form given in equation (79b).) In keeping with the previous analysis, this function of x will be denoted by $f(x)$ if it is determined from linear theory and by $g(x)$ if determined from transonic theory.

Although the linear-theory approximation is unsatisfactory at $M_\infty=1$, the same intuitive procedure can be extended to sonic flow. The desired expression follows if $\varphi_{B,t}$ is determined from the transonic differential equation. Thus, as given in equation (85), one has to a known order of accuracy,

$$\varphi_W=\varphi_{2_{W,\alpha}}+\varphi_{2_{W,t}}-\varphi_{2_{B,t}}+\varphi_{B,t} \tag{90}$$

and this result reduces for points near the body to

$$\varphi_W=\varphi_{2W}+g(x) \tag{91}$$

where

$$\varphi_{2_W}=\varphi_{2_{W\alpha}}+\varphi_{2_{W,t}},\quad g(x)=\lim_{r\to 0}(\varphi_{B,t}-\varphi_{2_{B,t}}) \tag{92}$$

as indicated in figure 6. It is apparent that equation (90) has a dual basis for validity and represents either the relation afforded by transonic theory for $M_\infty=1$, or that given by linear theory for other Mach numbers. The customary restriction to slender wings and bodies must be observed in both applications.

The power and weakness of the present intuitive reasoning is well illustrated by the fact that the relation given by equation (90) is found without recourse to the detailed investigation of the earlier sections whereas the restriction to small angles of attack that enters in the simplification is overlooked. This deficiency stems from the fact that it is insufficient to assure that merely the infinite velocities be removed. Since the space involved is infinite, it is also necessary that certain integrals of velocity (see eq. (43)) be finite, and it is in connection with the attenuation of the velocities arising from the term $\varphi_{2_{W,\alpha}}$ that the deficiency occurs. One could, perhaps, have continued the heuristic reasoning but, once the principal idea has been established, formal analysis can be used to establish the restrictions and to evaluate the error terms involved.

Some insight into the validity of the foregoing equations can be obtained by examining the numerical solution given by Yoshihara in reference 17 for sonic flow about a circular cone-cylinder at zero angle of attack. Inasmuch as it was not assumed either explicitly or implicitly that the perturbation potential in the vicinity of the body has the form indicated by equation (91) (the boundary conditions were satisfied at the actual body surface rather than along the body axis), these results are particularly suited in this respect for the investigation of the region for which the simplified relation applies. On the other hand, the example is not ideal because the sharp corner at the shoulder violates the smoothness condition; it is, however, the only case for which a theoretical solution is available. Accordingly, figure 7 has been prepared so as to show the variation of

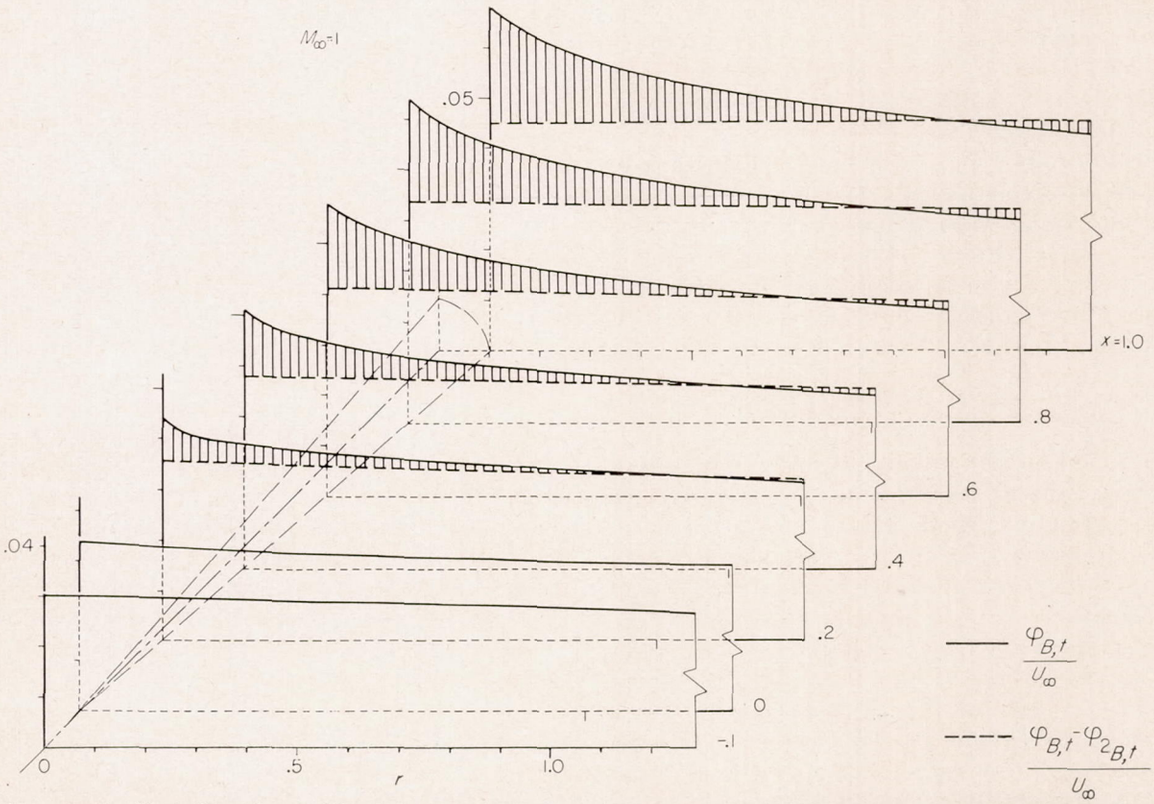

FIGURE 7.—Variation of $\varphi_{B,t}/U_\infty$ with r for several stations along the length of a cone-cylinder of semiapex angle 1/10 at free-stream Mach number 1.

$\varphi_{B,t}/U_\infty$ with r for several stations along the length of the cone for the case in which the semiapex angle θ is 1/10 radian. Attention is called to the fact that the values for $\varphi_{B,t}$ given in this figure are for a cone of unit length whereas the original values given in figure 5 of reference 17 are for a cone of length 10. A dotted line is also shown for each station representing the values obtained after subtracting $\varphi_{2_{B,t}}/U_\infty$ computed by

$$\frac{\varphi_{2_{B,t}}}{U_\infty}=\frac{1}{2\pi}\frac{dS}{dx}\,lnr=\frac{xlnr}{100} \tag{93}$$

from $\varphi_{B,t}/U_\infty$ at the same point. In order to illustrate further the nature of these results, figure 8 has been prepared

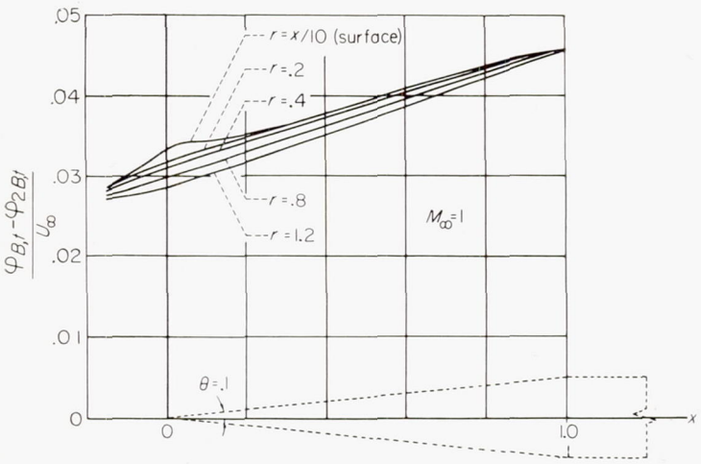

FIGURE 8.—Variation of $\varphi_{B,t}-\varphi_{2_{B,t}}$ with x for several r of a cone-cylinder of semiapex angle 1/10 at free-stream Mach number 1.

to show the variation of $\varphi_{B,t}-\varphi_{2_{B,t}}$ with x for various r. The resulting values should, according to equation (92), be a function of x alone for small r. It can be seen from an examination of these figures that the difference $\varphi_{B,t}-\varphi_{2_{B,t}}$ is indeed very nearly a function of x in most of the region for which results are available. Slight deviations occur in the immediate vicinity of the nose and at the largest distances from the body. The latter departures are so small, however, that it is necessary to possess additional information for greater distance from the body before one can determine the extent of the region for which the $g(x)$ function is applicable.

DETERMINATION OF $g'(x)$ IN TERMS OF PRESSURE DISTRIBUTION ON A NONLIFTING BODY OF REVOLUTION

Although $\varphi_{B,t}$, and hence $f(x)$, can be calculated directly by means of linear theory for either distinctly subsonic or supersonic flow, general methods are not yet available for the theoretical determination of $\varphi_{B,t}$ in transonic theory. It is evident from its definition, however, that $g(x)$ depends only on the longitudinal distribution of cross-section area $S(x)$, and that its derivative can be determined from simple aerodynamic measurements of the flow about a slender nonlifting body of revolution having the same $S(x)$ as the given body. From the point of view of applications, nothing is lost in not knowing the actual level of $g(x)$, however, since knowledge of its gradient, $g'(x)$, is sufficient for the determination of flow quantities such as velocity and pressure. Since the easiest flow quantity to measure is generally the pressure distribution on the surface of the body, perhaps the simplest way to determine $g'(x)$ is through a relation expressing this quantity in terms of the pressure distribution. The necessary relations for the perturbation velocity potential, $\varphi_{B,t}$ and the pressure coefficient $C_{p_{B,t}}$ are provided by equations (48) and (5), which reduce, in the vicinity of a slender nonlifting body of revolution, to

$$\varphi_{B,t}=\frac{U_\infty}{2\pi}\frac{dS}{dx}\,lnr+g(x) \tag{94}$$

$$(C_{p_{B,t}})_{r=R}=-\frac{2}{U_\infty}\frac{\partial}{\partial x}\varphi_{B,t}-\left(\frac{dR}{dx}\right)^2=-\frac{2}{U_\infty}\frac{\partial}{\partial x}\varphi_{B,t}-\frac{S'^2(x)}{4\pi S} \tag{95}$$

where $R(x)$ represents the radius of the body of revolution and the prime denotes differentiation with respect to x. These relations can be combined to solve for $g'(x)$ in terms of the surface pressures and the cross-section area with the following result:

$$g'(x)=-\frac{U_\infty}{2}\left[(C_{p_{B,t}})_{r=R}+\frac{S''(x)}{2\pi}\,ln\frac{S}{\pi}+\frac{S'^2(x)}{4\pi S}\right] \tag{96}$$

The cone-cylinder solution of Yoshihara (ref. 17) again affords a means of illustrating the application of this result at $M_\infty=1$. Thus, figure 9 has been prepared to illustrate the variations with x of the pressure coefficient [2] on the surface of a cone-cylinder having a semiapex angle of 1/10 radian, and of $g'(x)/U_\infty$ computed therefrom, using equation (96). As in the case of figures 7 and 8, the values of $g'(x)$ have been converted from those given originally for a cone of length 10 to those for a cone of unit length.

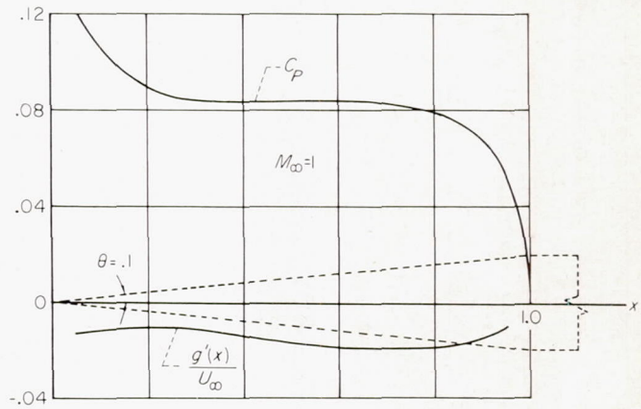

FIGURE 9.—Variation of C_p and $g'(x)$ on the surface of a cone-cylinder of semiapex angle 1/10 at free-stream Mach number 1.

It is likewise evident that the function $g'(x)$ can also be determined from pressure-distribution data for thin wings in an analogous manner, although naturally more geometric quantities are involved in the calculation.

[2] The curve for $C_{p_{B,t}}$ shown in figure 9 differs from that given originally in reference 17 due to the correction of a sign error in the quadratic term of the expression for pressure coefficient. For the cone having a semiapex angle of 1/10 radian, this change has the effect of diminishing the values given originally for $C_{p_{B,t}}$ on the cone surface by a constant amount, namely, 0.02.

RELATION BETWEEN PRESSURE DISTRIBUTIONS ON RELATED WINGS AND BODIES

Wings and bodies having same longitudinal distribution of cross-section area.—Equation (90) displays the relationship between the perturbation velocity potential φ_W for a thin low-aspect-ratio wing and the corresponding potential $\varphi_{B,t}$ for a slender nonlifting body of revolution having the same longitudinal distribution of cross-section area. In most practical applications, however, one is not so much interested in relations involving the velocity potential as those involving the pressure distributions. The following discussion will be concerned with the derivation of such a relation. Thus, consider the two objects illustrated in figure 10. Both have the same $S(x)$, but the first is a non-

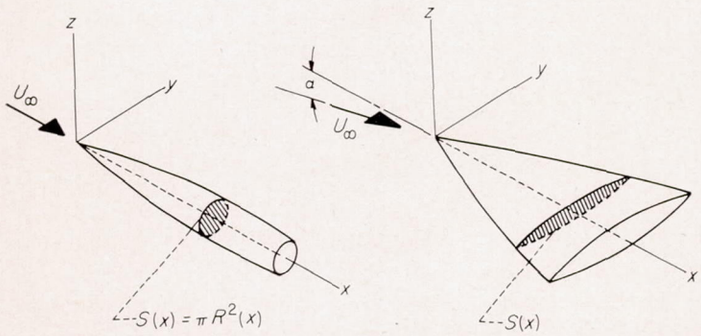

FIGURE 10.—Views of wing and body having the same longitudinal distribution of cross-section area.

lifting body of revolution and the second is a thin lifting wing. The relations for the potential and pressure coefficient for the body of revolution are those given in equations (94) and (95) of the preceding section. The corresponding relations for φ_W and C_{p_W} in the vicinity of the wing are

$$\varphi_W=\varphi_{2_W}+g(x) \tag{97}$$

$$C_{p_W}=-\frac{2}{U_\infty}\frac{\partial\varphi_W}{\partial x} \tag{98}$$

Since $g(x)$ is the same for both objects, the desired relation between the pressure distributions on the wing and body of revolution can be determined by combining equations (95) through (98); thus

$$C_{p_W}=(C_{p_{B,t}})_{r=R}-\frac{2}{U_\infty}\frac{\partial\varphi_{2_W}}{\partial x}+\frac{S''(x)}{2\pi}\ln\frac{S}{\pi}+\frac{S'^2(x)}{4\pi S} \tag{99}$$

It is interesting to note that this relation holds not only for nonlinear theory of sonic flow, but also for linearized slender-body theory for subsonic and supersonic flow. This follows directly from the fact that equation (91) and the associated statement are equally correct in linearized slender-body theory if $g(x)$ is replaced by $f(x)$.

The term involving φ_{2_W} can be considered known inasmuch as it can be determined directly using equation (50) or any of several other methods (e. g., conformal mapping, etc.) available from classical two-dimensional potential theory, or indirectly if either the linear theory or the slender-wing-theory solutions are known for the wing. To illustrate, let the subscript S denote the values indicated by the slender-wing-theory solution. Then, for example, if $(\varphi_W)_s$ is known, φ_{2_W} is given by

$$\varphi_{2_W}=(\varphi_W)_s-f(x) \tag{100}$$

where $f(x)$ is provided by equations (79). Correspondingly, one has

$$-\frac{2}{U_\infty}\frac{\partial\varphi_{2_W}}{\partial x}=(C_{p_W})_S+\frac{2}{U_\infty}f'(x) \tag{101}$$

If, on the other hand, the linear-theory solution is available, the relation

$$\lim_{M_\infty\to 1}\varphi_L=\lim_{M_\infty\to 1}\varphi_S \tag{102}$$

applies, whence

$$-\frac{2}{U_\infty}\frac{\partial\varphi_{2_W}}{\partial x}=\lim_{M_\infty\to 1}\left[(C_{p_W})_L+\frac{2}{U_\infty}f'(x)\right] \tag{103}$$

where the subscript L refers to values given by linear theory.

Equation (99) enables one to calculate the pressures in the vicinity of any thin low-aspect-ratio wing, provided the pressure distribution is known on the surface of a nonlifting body of revolution having the same longitudinal distribution of cross-section area $S(x)$. The corresponding rule relating the pressures on two wings having different cross-section shapes but the same $S(x)$ can be easily derived by applying equation (99) twice and subtracting so as to eliminate all terms pertinent to the body of revolution..

Wings and bodies having similar longitudinal distribution of cross-section area.—It is a simple matter to extend the previous results so as to include more general relations which apply to wings and bodies having longitudinal distributions of cross-section area that are merely proportional. The information needed to achieve this generalization is supplied by the transonic similarity rule for slender bodies of revolution (ref. 5). The rule states that at $M_\infty=1$ the pressure distributions on two slender bodies of revolution having area distributions given by

$$S_{\mathrm{II}}\left(\frac{x}{l}\right)=\frac{S_{m,\mathrm{II}}}{S_{m,\mathrm{I}}}S_{\mathrm{I}}\left(\frac{x}{l}\right) \tag{104}$$

are related according to

$$C_{p_{B,\mathrm{II}}}\left(\frac{x}{l}\right)=\frac{S_{m,\mathrm{II}}}{S_{m,\mathrm{I}}}C_{p_{B,\mathrm{I}}}\left(\frac{x}{l}\right)+\frac{1}{\pi}\frac{d^2S_{\mathrm{II}}(x/l)}{d(x/l)^2}\ln\frac{S_{m,\mathrm{I}}}{S_{m,\mathrm{II}}}\left(\frac{\gamma_{\mathrm{I}}+1}{\gamma_{\mathrm{II}}+1}\right)^{1/2} \tag{105}$$

where S_m refers to the maximum cross-section area and the subscripts I and II refer to properties associated with the two bodies. If both bodies are in air, $\gamma_{\mathrm{I}}=\gamma_{\mathrm{II}}$, and equation (105) reduces to

$$C_{p_{B,\mathrm{II}}}\left(\frac{x}{l}\right)=\frac{S_{m,\mathrm{II}}}{S_{m,\mathrm{I}}}C_{p_{B,\mathrm{I}}}\left(\frac{x}{l}\right)+\frac{1}{\pi}\frac{d^2S_{\mathrm{II}}(x/l)}{d(x/l)^2}\ln\frac{S_{m,\mathrm{I}}}{S_{m,\mathrm{II}}} \tag{106}$$

If it is desired to determine the pressures C_{p_W} for a wing having an area distribution given by $S_{\mathrm{II}}(x/l)$ and the pressure distribution is known for a body of revolution having an area distribution $S_{\mathrm{I}}(x/l)$ proportional to $S_{\mathrm{II}}(x/l)$, one merely computes $C_{p_{B,\mathrm{II}}}$ for a body of revolution of area $S_{\mathrm{II}}(x/l)$ using equation (106) and substitutes the result for $C_{p_{B,t}}$ in equation (99).

APPLICATION TO THE CALCULATION OF PRESSURES AND FORCES ON THIN ELLIPTIC CONE-CYLINDERS AT $M_\infty=1$

The relations developed in the preceding section will now be applied to the calculation of the pressures and forces at $M_\infty=1$ on the conical portion of the thin cone-cylinder of

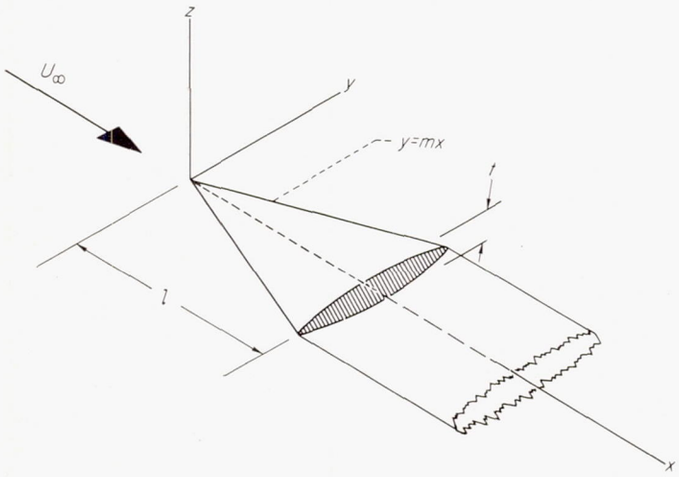

FIGURE 11.—View of thin elliptic cone-cylinder.

elliptic cross-section illustrated in figure 11. The ordinates of the upper surface of the cone are given by

$$z_u(x,y)=\frac{t}{2ml}\,(m^2x^2-y^2)^{1/2} \tag{107}$$

where m is the tangent of the semiapex angle, l is the length of the cone, and t is the maximum thickness of the cone. It follows that the elliptic section in the plane $x=x_1$ has major and minor semiaxes equal to mx_1 and $tx_1/2l$, respectively. The cross-section area and surface slope are, respectively,

$$S(x_1)=\frac{\pi t m x_1^2}{2l},\quad \frac{\partial z_u}{\partial x_1}=\frac{mtx_1}{2l(m^2x_1^2-y^2)^{1/2}} \tag{108}$$

Pressure distribution on nonlifting cone-cylinders.—From equation (50), φ_{2_W} for the symmetrical nonlifting case can be written as

$$\varphi_{2_W}=\frac{1}{2\pi}\int_{-mx}^{mx} 2U_\infty\,\frac{\partial z_u}{\partial x}\,(x,y_1)\,ln[(y-y_1)^2+z^2]^{1/2}dy_1 \tag{109}$$

which, when evaluated on the wing surface (i. e., $z=0$, $-mx<y<mx$), yields

$$\varphi_{2_W}=\frac{U_\infty tmx}{2l}\,ln\,\frac{mx}{2} \tag{110}$$

After inserting this relation into equation (99) and carrying out the indicated operations, one obtains

$$C_{p_W}=C_{p_B}-\frac{mt}{2l}\left(1+ln\,\frac{ml}{2t}\right) \tag{111}$$

where C_{p_B} refers to the pressure distribution on a circular cone-cylinder having such a semiapex angle θ that it has the same longitudinal distribution of cross-section area as the elliptic cone-cylinder; thus

$$\theta=\left(\frac{mt}{2l}\right)^{1/2}$$

The pressures on such a body can be determined from those shown graphically in figure 9 for $\theta=0.10$ by application of equation (106), which reduces to the form

$$C_{p_B}=100\theta^2(C_{p_B})_{\theta=0.10}-2\theta^2 ln100\theta^2 \tag{112}$$

As mentioned previously, following equation (99), the difference $C_{p_W}-C_{p_B}$ is the same as given by linearized slender-body theory for subsonic or supersonic flow. As a corroboration of this statement, consider the expression given by slender-body theory for the supersonic pressure on the thin elliptic cone (ref. 25, p. 257)

$$C_{p_{SW}}=-\frac{mt}{l}\left[1+ln\,\frac{m(M_\infty^2-1)^{1/2}}{4}\right] \tag{113}$$

and the corresponding expression for the supersonic pressure distribution on the slender circular cone (ref. 25, p. 241)

$$\begin{aligned}C_{p_{SB}}&=-\theta^2\left[1+2ln\,\frac{\theta(M_\infty^2-1)^{1/2}}{2}\right]\\&=-\frac{mt}{2l}\left\{1+2ln\left[\frac{mt(M_\infty^2-1)}{8l}\right]^{1/2}\right\}\end{aligned} \tag{114}$$

The difference between equations (113) and (114) obviously reduces to the form given in equation (111).

The application of the foregoing theory to a specific case will now be illustrated by determining the pressure distribution C_{p_W} at $M_\infty=1$ on an elliptic cone having $m=1/2$ and $t/l=0.06$. The first step is to calculate the pressure distribution at $M_\infty=1$ on the surface of a circular cone-cylinder having a semiapex angle given by

$$\theta=\left(\frac{mt}{2l}\right)^{1/2}=(0.015)^{1/2}=0.1225 \tag{115}$$

The pressure distribution on the selected elliptic cone-cylinder can then be calculated through use of equation (111) and is

$$C_{p_W}=C_{p_B}-0.0364 \tag{116}$$

The results for both the circular and the elliptic cone-cylinders are shown graphically in figure 12. Note that the pressure distribution is independent of y in this case and that a single curve of C_{p_W} versus x/l suffices to define the pressure on the wing.

Drag of nonlifting cone-cylinders.—The drag D_W at $M_\infty=1$ of thin elliptic cone-cylinders can be obtained by direct integration of the product of the pressure and surface slope and is expressible in the form

$$D_W=D_e+\frac{\rho_\infty U_\infty^2}{2}\iint_W 2C_{p_W}\,\frac{\partial z_u}{\partial x}\,dxdy \tag{117}$$

where the integration is extended over the plan form and D_e represents the contribution to the drag that results from a finite leading-edge radius of curvature. Since only that portion of φ_W denoted by φ_{2_W} contributes to D_e, this quantity can be calculated in the same manner as described in references 25 and 28 for linear theory. Thus, the contribution per unit of span is, in slender theory,

$$\frac{dD_e}{dy}=\pi\,\frac{\rho_\infty U_\infty^2}{2}\,r_n\left(\frac{ds}{dx}\right)^2 \tag{118}$$

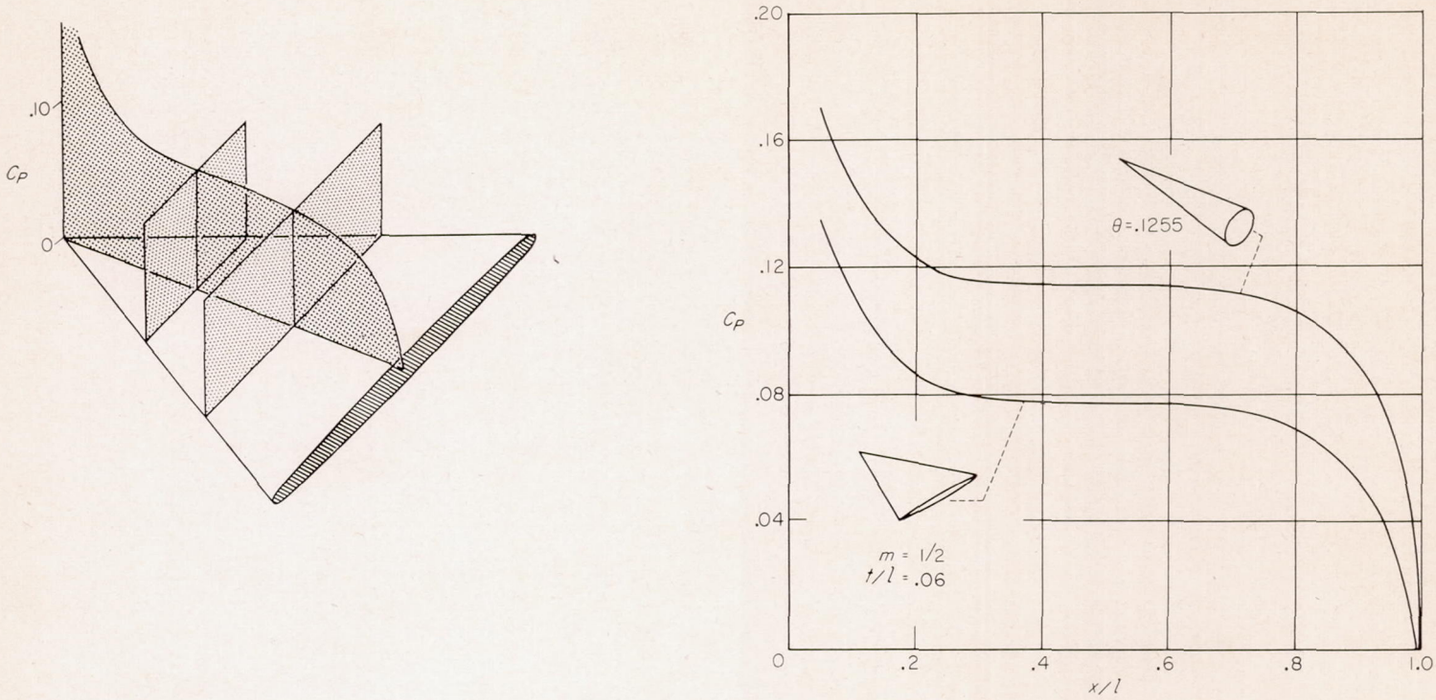

FIGURE 12.—Pressure distribution on a thin elliptic cone-cylinder at free-stream Mach number 1.

where r_n is the radius of curvature normal to the wing leading edge and s is the local semispan. If the ordinate of the wing, in the vicinity of the leading edge, is

$$z_u = h(s,y)(s-y)^{1/2} \tag{119}$$

equation (118) becomes

$$\frac{dD_e}{dy} = \frac{\pi}{2}\frac{\rho_\infty U_\infty^2}{2} h^2(s,s)\left(\frac{ds}{dx}\right)^2 \tag{120}$$

For the thin elliptic cone, z_u is given by equation (107) and $s(x)=mx$, hence

$$h^2(s,s) = \frac{st^2}{2m^2l^2}$$

and

$$D_e = 2\int_0^l \frac{dD_e}{dy}\, m\, dx = \frac{\pi}{4}\frac{\rho_\infty U_\infty^2}{2} m^2t^2 \tag{121}$$

The second term on the right of equation (117) becomes, upon substitution of equation (111) for C_p

$$\frac{\rho_\infty U_\infty^2}{2}\iint_W 2C_{p_W}\frac{\partial z_u}{\partial x}\,dx\,dy = \frac{\rho_\infty U_\infty^2}{2}\left[\int_0^l C_{p_B}\frac{dS}{dx}\,dx - \frac{mt}{2l}\left(1+ln\frac{ml}{2t}\right)S(l)\right]$$
$$= D_B - \frac{\pi}{4}\frac{\rho_\infty U_\infty^2}{2} m^2t^2\left(1+ln\frac{ml}{2t}\right)$$

The drag of the elliptic cone-cylinder is thus

$$D_W = D_B - \frac{\pi}{4}\frac{\rho_\infty U_\infty^2}{2} m^2t^2\, ln\frac{ml}{2t} \tag{122}$$

Note that the circular cone-cylinder and elliptic cone-cylinder have different values of drag at $M_\infty=1$, even though they have the same area distribution. As an illustration of the order of magnitude of the quantities involved in equation (122), the drag at $M_\infty=1$ of a circular cone-cylinder having semiapex angle $\theta=0.1225$, as determined by integration of the pressure distribution shown in figure 12, is

$$(D_B)_{\theta=0.1225} = 0.00484\frac{\rho_\infty U_\infty^2}{2} l^2 \tag{123}$$

whereas that of an elliptic cone-cylinder having $m=1/2$ and $t/l=0.06$ is

$$(D_W)_{\substack{m=1/2\\ t/l=0.06}} = 0.00383\frac{\rho_\infty U_\infty^2}{2} l^2 \tag{124}$$

Thus, although both bodies have the same area distribution, the drag of the elliptic cone-cylinder is less than 80 percent of that of the circular cone-cylinder.

More general results for circular and elliptic cone-cylinders can be obtained by combining equations (123) and (124) with the transonic similarity rule for the drag of slender bodies of revolution. The latter can be derived by integration of the corresponding relation for the pressure given in equation (106) and was first given by Oswatitsch and Berndt in reference 5. It states that the drags at $M_\infty=1$ of two bodies of revolution having area distributions given by equation (104) are related assuming both bodies are in air, so that $\gamma_{\mathrm{I}}=\gamma_{\mathrm{II}}$, according to

$$D_{\mathrm{II}} = \left(\frac{S_{m,\mathrm{II}}}{S_{m,\mathrm{I}}}\right)^2\left[D_{\mathrm{I}} + \frac{\rho_\infty U_\infty^2}{2}\frac{S_{\mathrm{I}}'^2(l) - S_{\mathrm{I}}'^2(0)}{2\pi}\, ln\frac{S_{m,\mathrm{I}}}{S_{m,\mathrm{II}}}\right] \tag{125}$$

For slender circular cone-cylinders $S=\pi\theta^2x^2$ and equation (125) reduces to

$$D_{\mathrm{II}}=\left(\frac{\theta_{\mathrm{II}}}{\theta_{\mathrm{I}}}\right)^4\left[D_{\mathrm{I}}+2\pi\frac{\rho_\infty U_\infty^2}{2}\theta_I^4 l^2 ln\left(\frac{\theta_{\mathrm{I}}}{\theta_{\mathrm{II}}}\right)^2\right] \tag{126}$$

which becomes, upon substitution of the values given by equation (123) for D_{I} and θ_{I}

$$D_B=-\pi\theta^4[1.55+2\,ln\,\theta^2]\frac{\rho_\infty U_\infty^2}{2}l^2 \tag{127}$$

The general expressions for D_W and D_B can be compared more readily if the relation $\theta=(mt/2l)^{1/2}$ is introduced to express θ in terms of m, t, and l of the thin elliptic cone having the same area distribution, thus

$$D_B=-\frac{\rho_\infty U_\infty^2}{2}\left[\frac{\pi}{4}m^2t^2\left(1.55+2\,ln\frac{mt}{2l}\right)\right] \tag{128}$$

Combination of equations (128) and (122) yields the corresponding result for the drag at $M_\infty=1$ of thin elliptic cone-cylinders

$$D_W=-\frac{\rho_\infty U_\infty^2}{2}\left[\frac{\pi}{4}m^2t^2\left(1.55+ln\frac{m^3t}{8l}\right)\right] \tag{129}$$

Before leaving the subject of similarity rules, it is of interest to note that equation (129) for the pressure drag of thin elliptic cone-cylinders is in accord with the transonic similarity rule for the pressure drag of thin wings of finite span (see, e. g., ref. 4). The latter is usually given in dimensionless form and provides that the pressure drag coefficient C_D at $M_\infty=1$ of a family of thin nonlifting wings of affinely related geometry, plan-form area S_p, thickness ratio τ, and aspect ratio A satisfy the equation

$$\frac{C_D}{\tau^{5/3}}=f(A\tau^{1/3}) \tag{130}$$

where

$$C_D=\frac{D_W}{\frac{\rho_\infty U_\infty^2}{2}S_p} \tag{131}$$

and f indicates a functional dependence. If indeterminate forms that arise from the infinite plan-form area of a cone-cylinder are avoided by letting S_p represent the plan-form area of only the conical part of the body, S_p, A, and τ are related to m, t, and l according to

$$S_p=ml^2,\quad A=4m,\quad \tau=\frac{t}{l} \tag{132}$$

and equation (129) can be rewritten as follows

$$\frac{C_D}{\tau^{5/3}}=\frac{D_W}{\frac{\rho_\infty U_\infty^2}{2}S_p\tau^{5/3}}=-\frac{\pi}{16}A\tau^{1/3}\left(1.55+3\,ln\frac{A\tau^{1/3}}{8}\right) \tag{133}$$

It is evident from this form of the result that $C_D/\tau^{5/3}$ is a function of $A\tau^{1/3}$ alone, as required by the similarity rule.

Pressures and forces on lifting cone-cylinders.—The relations summarized in figure 6 also permit the calculation of the pressure distribution on a thin elliptic cone-cylinder when inclined at a small angle of attack. To calculate this quantity, one must first have the expression for $\varphi_{2_{W,\alpha}}$. The necessary expression is well known, however, since the problem is equivalent mathematically, for the planar boundary conditions, to the boundary-value problem associated with translation of a flat plate in a two-dimensional incompressible fluid. Thus $\varphi_{2_{W,\alpha}}$ and φ_{2_W} on the surface of the thin inclined elliptic cone are

$$\varphi_{2W,\alpha}=\pm U_\infty\alpha(m^2x^2-y^2)^{1/2} \tag{134}$$

$$\varphi_{2W}=\frac{U_\infty tmx}{2l}\,ln\,\frac{mx}{2}\pm U_\infty\alpha(m^2x^2-y^2)^{1/2} \tag{135}$$

where the upper (plus) sign is to be used on the upper surface and the lower (minus) sign on the lower surface. After inserting equation (135) into equation (99), one obtains

$$C_{p_W}=C_{p_B}-\frac{mt}{2l}\left(1+ln\frac{ml}{2t}\right)\mp\frac{2\alpha m^2x}{(m^2x^2-y^2)^{1/2}} \tag{136}$$

where the convention concerning upper and lower signs still holds. The aerodynamic loading, or the difference in pressure between the two sides of the wing, is thus

$$\frac{\Delta p_W}{\rho_\infty U_\infty^2/2}=(C_{p_W})_l-(C_{p_W})_u=\frac{4\alpha m^2x}{(m^2x^2-y^2)^{1/2}} \tag{137}$$

A sketch of the load distribution is shown in figure 13. Integration of the loading over the plan form leads to the following expression for lift

$$L_W=\frac{\rho_\infty U_\infty^2}{2}(2\pi\alpha m^2l^2) \tag{138}$$

Although the pressure distribution at $M_\infty=1$ is not the same as given by linear theory, it will be recognized that the load distribution and lift arise solely from $\varphi_{2_{W,\alpha}}$ and are there-

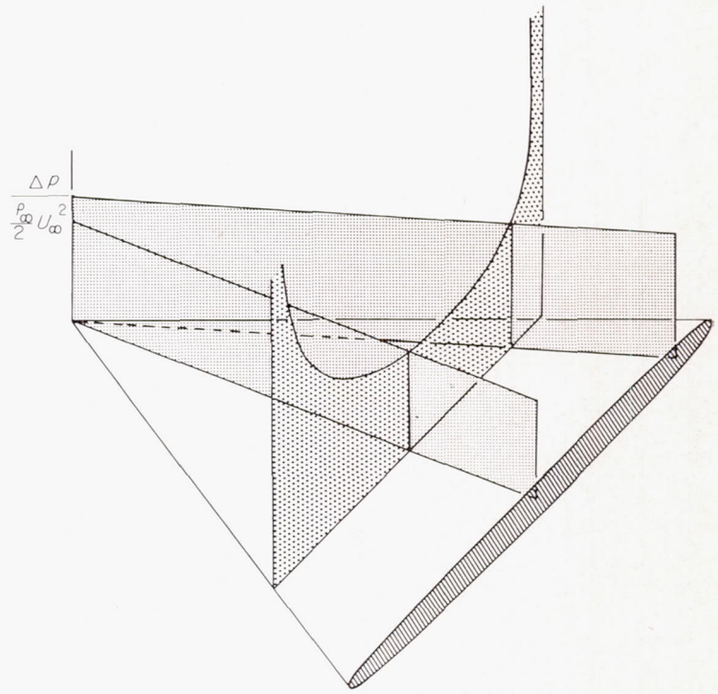

FIGURE 13.—Load distribution on an inclined thin elliptic cone-cylinder.

fore the same as given by linear slender-wing theory. One recognizes, consequently, that the lift of any low-aspect-ratio wing having such a plan form that no part of the trailing edge extends forward of the station of maximum span is given by

$$L_W=\frac{\rho_\infty U_\infty^2}{2}(2\pi\alpha s_0^2) \tag{139}$$

and the drag due to lift by

$$D_W-D_{W_{\alpha=0}}=\frac{\alpha}{2}L \tag{140}$$

The fraction ½ enters as a result of suction forces on the leading edge. Note that the above statements also imply that all reciprocal and reverse flow relations of linear theory are applicable to lifting forces at $M_\infty=1$ on slender wings at small angles of attack.

As in the case of drag discussed previously, equation (138) for the lift of thin low-aspect-ratio wings is compatible with the transonic similarity rule which states that the lift-curve slopes of a family of thin wings of finite span and affinely related geometry are related according to (see, e. g., ref. 4)

$$\tau^{1/3}C_{L_\alpha}=f(A\tau^{1/3}) \tag{141}$$

where

$$C_{L_\alpha}=\lim_{\alpha\to 0}\frac{L}{(\rho_\infty U_\infty^2/2)S_p\alpha} \tag{142}$$

Substitution of the geometric relations of equation (132) into equation (138) for the lift, yields simply

$$\tau^{1/3}C_{L_\alpha}=\frac{\pi}{2}A\tau^{1/3} \tag{143}$$

which is obviously in accord with the similarity rule. The drag due to lift given by equation (140) is in corresponding agreement with the appropriate transonic similarity rule.

MOMENTUM ANALYSIS OF DRAG OF SLENDER BODIES AT $M_\infty=1$

The previous example of the thin elliptic cone-cylinder has disclosed significant differences in the drag at $M_\infty=1$ of elliptic and circular cone-cylinders having the same longitudinal distribution of cross-section area. Since this finding is contrary to the often quoted transonic area rule, it is of interest to study the sonic drag of a more general class of bodies. This will now be done using momentum methods.

Derivation of general relation for drag.—Consider a surface Σ which encloses a volume containing an aerodynamic body. The vectorial force F on the body can be determined by considering the pressures and flux of momentum at Σ. In general there results

$$\vec{F}=-\iint_\Sigma (p-p_\infty)d\vec{\Sigma}-\iint_\Sigma \rho\vec{V}\left[\left(\vec{U}_\infty+\vec{V}\right)\cdot d\vec{\Sigma}\right] \tag{144}$$

where vector notation is used, p and ρ are the local static pressure and density, and $\vec{V}$ is the local perturbation velocity vector.

For present purposes, the surface Σ will be taken as shown in figure 14. Two parts of Σ denoted as I and II, are plane

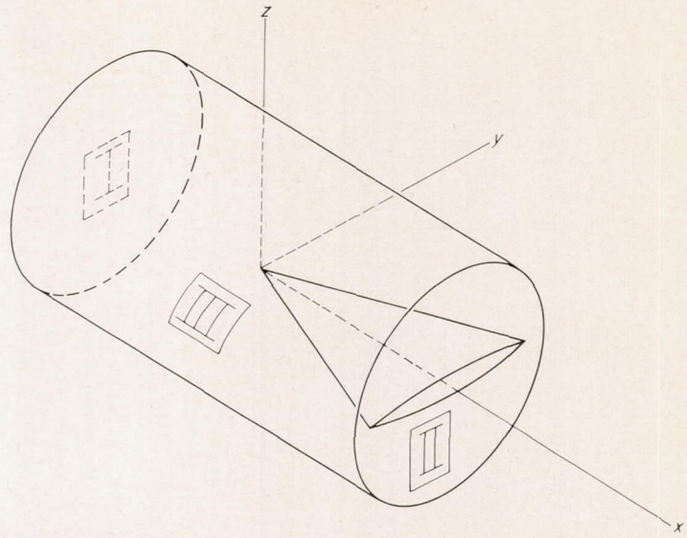

FIGURE 14.—View of surface Σ used in evaluation of drag.

surfaces normal to the x axis and situated upstream and downstream of the body. The remaining part of Σ, denoted by III, is a small circular cylinder of radius R_Σ large enough so that the body is entirely enclosed within the cylindrical surface. Since it will be assumed that the body is slender and smooth enough that the necessary restrictions on φ are satisfied at all stations forward of the base, but that discontinuities in geometry or velocity may occur there, the plane surfaces I and II will be placed at infinity upstream and at the base of the body, respectively.

It is sufficient, to the order of accuracy of transonic theory, to approximate p and ρ at points near the body by

$$\frac{\rho}{\rho_\infty}=1-\frac{M_\infty^2 u}{U_\infty}$$

and

$$p-p_\infty=-\rho_\infty\left\{U_\infty u+\frac{1}{2}[(1-M_\infty^2)u^2+v_2+w^2]\right\}$$

Furthermore, if attention is restricted to the streamwise component of force, total drag of the enclosed body is given by

$$D=\frac{\rho_\infty}{2}\iint_{\mathrm{II}}[(M_\infty^2-1)u^2+v^2+w^2]\,dy\,dz-\rho_\infty\iint_{\mathrm{III}}uv_rR_\Sigma d\theta\,dx \tag{145}$$

where v_r is the radial component of velocity. This expression holds, of course, at $M_\infty=1$ and becomes

$$D=\frac{\rho_\infty}{2}\iint_{\mathrm{II}}(v^2+w^2)dy\,dz-\rho_\infty\iint_{\mathrm{III}}uv_rR_\Sigma d\theta\,dx \tag{146}$$

An alternative form for equation (146) which will prove useful can be obtained by replacing the surface integral over II by a line integral. Thus, Green's theorem provides

$$\begin{aligned}\iint_{\mathrm{II}}(v^2+w^2)dy\,dz&=\iint_{\mathrm{II}}\left[\left(\frac{\partial\varphi}{\partial y}\right)^2+\left(\frac{\partial\varphi}{\partial z}\right)^2\right]dy\,dz\\&=-\int_C\varphi\frac{\partial\varphi}{\partial n}d\sigma_c-\iint_{\mathrm{II}}\varphi\nabla^2\varphi\,dy\,dz\end{aligned} \tag{147}$$

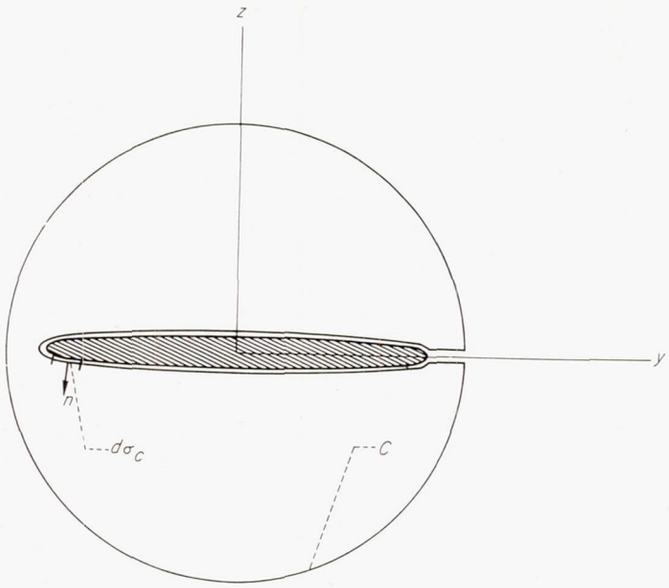

FIGURE 15.—View of integration contour in plane II of Σ.

where C is a curve, situated in plane II, which goes around the wing and also around the control surface Σ, $d\sigma_c$ is an element of C, and n is the unit normal drawn into the interior of C, as illustrated in figure 15. But the relation $\varphi=\varphi_2+g(x)$ holds near the body, and therefore within C, hence the equation $\nabla^2\varphi=0$ is satisfied in II,

$$\iint_{\mathrm{II}}(v^2+w^2)dy\,dz=-\int_C\varphi\frac{\partial\varphi}{\partial n}d\sigma_c \tag{148}$$

and equation (146) for drag becomes

$$D=-\frac{\rho_\infty}{2}\int_C\varphi\frac{\partial\varphi}{\partial n}d\sigma_c-\rho_\infty\iint_{\mathrm{III}}uv_rR_\Sigma d\theta\,dx \tag{149}$$

Relation between drag of wings and bodies having the same area distribution.—Consider sonic flow about two aerodynamic shapes, one a thin wing and the other a slender nonlifting body of revolution, having the same longitudinal distribution of cross-section area. If equations (90) and (91) are substituted into equation (146), and if the Fourier expansion for $\varphi_{2_W}-\varphi_{2_B}$ obtained from equations (58) and (65) is introduced into the integrals over III and the portion of C contiguous with III, one has

$$D_W=-\frac{\rho_\infty}{2}\left[\int_{C_W}\varphi_{2_W}\frac{\partial\varphi_{2_W}}{\partial n}d\sigma_c+U_\infty\frac{dS}{dx}g(x)+\int_{C_{\mathrm{III}}}\varphi_B\frac{\partial\varphi_B}{\partial n}d\sigma_c\right]-\rho_\infty\iint_{\mathrm{III}}u_Bv_{r_B}R_\Sigma d\theta\,dx \tag{150}$$

The contour C is here divided into two parts. The inner portion that immediately surrounds the wing is denoted by C_W, whereas the outer portion is denoted by C_{III}. It follows similarly that a corresponding expression can be written for the drag of the body of revolution. Thus

$$D_B=-\frac{\rho_\infty}{2}\left[\int_{C_B}\varphi_{2_B}\frac{\partial\varphi_{2_B}}{\partial n}d\sigma_c+U_\infty\frac{dS}{dx}g(x)+\int_{C_{\mathrm{III}}}\varphi_B\frac{\partial\varphi_B}{\partial n}d\sigma_c\right]-\rho_\infty\iint_{\mathrm{III}}u_Bv_{r_B}R_\Sigma d\theta\,dx \tag{151}$$

where C_B refers to an integration contour drawn around the cross section of the body. If the exterior portions of the control surface Σ are now selected the same for the two cases (i. e., surface III is the same for the wing and body), it follows immediately by subtraction that

$$D_W=D_B-\frac{\rho_\infty}{2}\left(\int_{C_W}\varphi_{2_W}\frac{\partial\varphi_{2_W}}{\partial n}d\sigma_c-\int_{C_B}\varphi_{2_B}\frac{\partial\varphi_{2_B}}{\partial n}d\sigma_c\right) \tag{152}$$

The integrals over C_W can be divided into two parts after recalling that the analysis applies for small angles of attack and that φ_{2_W} can be written as the sum of $\varphi_{2_{W,t}}$ and $\varphi_{2_{W,\alpha}}$, provided the thickness does not vanish. Substitution of this relation into equation (152) yields

$$D_W=D_B-\frac{\rho_\infty}{2}\left(\int_{C_W}\varphi_{2_{W,\alpha}}\frac{\partial\varphi_{2_{W,\alpha}}}{\partial n}d\sigma_c+\int_{C_W}\varphi_{2_{W,t}}\frac{\partial\varphi_{2_{W,t}}}{\partial n}d\sigma_c-\int_{C_B}\varphi_{2_B}\frac{\partial\varphi_{2_B}}{\partial n}d\sigma_c\right) \tag{153}$$

where the integrals involving the cross-product terms are absent since $\varphi_{2_{W,t}}$ and its normal derivative along C_W are even functions of z, whereas $\varphi_{2_{W,\alpha}}$ and its normal derivative are odd functions of z.

Since $\varphi_{2_{W,\alpha}}$ is proportional to α, it is evident that the first integral of equation (153) provides a contribution to the drag which is proportional to the square of the angle of attack. This quantity is exactly the vortex drag and is represented by the same expression at all Mach numbers.

The difference of the two remaining integrals gives the difference in the drag at $M_\infty=1$ of a nonlifting wing and body having the same longitudinal distribution of cross-section area. Since the two integrals will not always cancel, the drag of the wing and body will, in general, be different. One can account in this way for the difference in drag of thin elliptic cone-cylinders and circular cone-cylinders disclosed previously by integration of surface pressures. To show this, one must evaluate the integrals of equation (152) at the shoulder of the cone-cylinder ($x=l$) using the expressions for φ_{2_W} and φ_{2_B} given in equations (110) and (93). In the integration, the contour C_W extends on both sides of the y axis from $-ml$ to $+ml$ whereas the contour C_B is a circle of radius θl. Upon carrying out the indicated operations, one obtains the same result as that given previously in equation (122) in which the drag of the elliptic cone-cylinder is substantially less than that of the circular cone-cylinder.

Special cases for which the drag of wing and body is the same.—Although it is important to note the difference in the drag of two bodies, it is perhaps even more important to know under what conditions the drag of the bodies is the same. If attention is confined to nonlifting cases so that $\varphi_{2_{W,\alpha}}$ is zero, the vortex drag vanishes, and the condition for the equality of the drag of a wing and body having the same area distribution is that the contribution of the last two integrals of equation (153) cancel. This condition is satisfied for certain large and important classes of shapes. One such class includes shapes that are cylindrical at the

base since, then,

$$\frac{\partial \varphi_{2_{W,t}}}{\partial n}=0, \qquad \frac{\partial \varphi_{2_B}}{\partial n}=0 \tag{154}$$

and

$$D_W=D_B \tag{155}$$

Another includes many shapes that taper to a point at the rear since, then, both integrals again vanish. Other classes for which it is more difficult to specify the geometry include shapes for which the integrals have equal values different from zero. The latter case provides some interesting situations in which some members of a family of wings and bodies having the same longitudinal distribution of cross-section area have the same drag and others have a different drag. To be more specific, consider a low-aspect-ratio pointed wing having a straight trailing edge normal to the free-stream direction and smooth airfoil sections closing with a finite wedge angle at the rear (an example of such a wing is a triangular wing with biconvex profiles), and a body of revolution having the same area distribution as the wing. Application of equation (153) to this pair of bodies quickly leads to the conclusion that the drag of the body of revolution is infinitely greater than that of the wing. This is apparent because the integral around the base of the wing is finite, whereas that around the base of the body is logarithmically infinite since

$$\int \varphi_{2_B} \frac{\partial \varphi_{2_B}}{\partial n} d\sigma_c=\frac{1}{2\pi}\left[\left(U_\infty \frac{dS}{dx}\right)^2 ln\, R\right]_{x=l} \tag{156}$$

and dS/dx is finite and R is zero at $x=l$. The infinite drag of this particular body of revolution is, of course, spurious and is no doubt associated with the fact that the round stern is too blunt to treat with a theory of the slender-body type. On the other hand, there is no reason to believe that the pressure drags of the wing and body are the same.

Since no corresponding difficulties occur at the base of the wing, let the drag of the above wing be compared with that of a second thin low-aspect-ratio wing having the same longitudinal area distribution. For such a comparison, equation (153) must be replaced by the corresponding relation between the drag of two wings

$$D_{W_{II}}=D_{W_I}-\frac{\rho_\infty}{2}\left(\int_{C_{W_{II}}} \varphi_{2_{W_{II}}} \frac{\partial \varphi_{2_{W_{II}}}}{\partial n} d\sigma_c-\int_{C_{W_I}} \varphi_{2_{W_I}} \frac{\partial \varphi_{2_{W_I}}}{\partial n} d\sigma_c\right) \tag{157}$$

It is immediately clear that the two wings have the same drag if they have the same geometry at the base. This condition for the equality of drag of two bodies having the same area distribution has been arrived at previously by Harder and Klunker (ref. 16) and by Berndt (ref. 29) by somewhat different means. As is apparent from the preceding discussion, this condition is sufficient but not necessary.

As a further example, consider the case where the geometry of the two wings is affinely related, that is, for a constant chord, the second wing is derived from the first by simple stretchings of the y and z dimensions. For the present class of wings, having straight trailing edges normal to the free-stream direction and airfoil sections closing with a finite wedge angle at the rear, each of the integrals of equation (157) can be written in the form

$$\int_{C_W} \varphi_{2_W} \frac{\partial \varphi_{2_W}}{\partial n} d\sigma_c=\int_{-1}^{1}\left[\varphi_{2_W}\, 2U_\infty \frac{\partial(z/t)}{\partial(x/l)}\right]_{x=l} s_0 \tau d\left(\frac{y}{s_0}\right) \tag{158}$$

Then the product $A\tau$ of aspect ratio and thickness ratio is the same for both wings, although A and τ individually may be different. It follows, moreover, from the fact that the ratio z/t of the wing ordinates to the maximum thickness is the same function of x/l and y/s_0 for affinely related wings, that φ_{2_W} is the same function of y/s_0 for both wings. Since s_0 is proportional to A and $A\tau$ is the same for both wings, it follows that the two integrals of equation (157) have the same value, and both wings have the same drag. Inasmuch as it is only the conditions at the trailing edge that enter into the integrals of equation (157), similar reasoning shows that the two wings also have the same drag if the condition of affinely related geometry applies only to the cross-section shape and surface slopes in the x direction at the trailing edge. On the other hand, if the wings have merely the same longitudinal distribution of cross-section area, the simple relations just described between the various elements of equation (157) no longer hold, and the wings will, in general, have different drags.

APPLICATION TO NONPLANAR PROBLEMS

Equation (90) expressing the relation between the perturbation potential for sonic flow about a thin low-aspect-ratio wing and that about a slender body of revolution has been derived on the assumption that the boundary conditions for the wing can be specified on a planar surface. The development outlined in figure 6 suggests that the result can actually be extended to include more general classes of slender shapes. Accordingly, assume that equation (90) holds for cases involving nonplanar boundary conditions and let the results given in the preceding sections for the drag at $M_\infty=1$ of thin elliptic cones be extended to include slender elliptic cones of any eccentricity. The analysis proceeds identically to that for the thin elliptic cone, the only change being that φ_{2_W} must be recalculated. This is a simple problem in two-dimensional potential theory since φ_{2_W} represents the potential associated with uniform growth of an ellipse, and the result, when evaluated on the cone surface, is

$$\varphi_{2_W}=\frac{U_\infty tmx}{2l}\, ln\left[\frac{mx}{2}\left(1+\frac{t}{2ml}\right)\right] \tag{159}$$

Substitution of this result into equation (153) leads to the following relation for the drag

$$D_W=D_B-\frac{\pi}{4}\frac{\rho_\infty U_\infty^2}{2} m^2t^2 ln\left[\frac{ml}{2t}\left(1+\frac{t}{2ml}\right)^2\right] \tag{160}$$

Comparison of these two expressions with the corresponding relations for thin cones given in equations (110) and (122) shows that they differ by the inclusion of an additional factor $(1+t/2ml)$ in the more general result. Although the contribution of this term is of negligible importance for cones having t/ml small, it is vital for nearly circular cones, and indeed necessary to assure the equality of D_W and D_B when the elliptic cone becomes a circular cone, that is, when $t/ml=2$. In order to illustrate this point further, figure 16 has been pre-

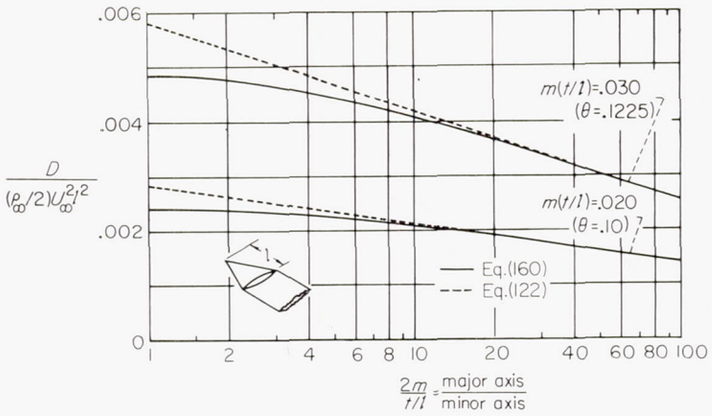

FIGURE 16.—Drag of elliptic cone-cylinders at free-stream Mach number 1.

pared, showing the variation with $2ml/t$, or the ratio of major axis to minor axis, of the drag at $M_\infty=1$ of two families of elliptic cones. All members of each family have the same longitudinal distribution of cross-section area. As indicated, one family is defined by $mt/l=0.02$ and includes the circular cone-cylinder having a semiapex angle θ of 0.10 radian, and the other by $mt/l=0.03$ and includes the circular cone-cylinder having $\theta=0.1225$ radian. The solid line indicates the values computed using equation (160), and the dotted line those computed using equation (122). In both cases, the drag D_B of the circular cone-cylinder is calculated from equation (127). As would be anticipated, the solid and dotted lines coincide for thin cones, but they differ considerably for circular cones ($2ml/t=1$). More interesting, perhaps, is the extent to which the drag of a family of cone-cylinders having the same longitudinal distribution of cross-section area depends on the shape of the cross section.

The procedures applied here to the elliptic cone-cylinders can also be applied to many other cases, such as wing-body combinations, etc. For bodies having the same longitudinal distribution of cross-section area as a cone-cylinder one must merely determine the appropriate function for φ_{2_W} and proceed in the same manner as for the elliptic cone-cylinders. For other bodies it is also necessary to have knowledge of either the theoretical solution or the experimental pressure distribution for sonic flow around a body of revolution having the same (or affinely related) longitudinal distribution of cross-section area as the given body. It should be remarked, however, that the extension to some of these problems involves the assumption that equation (90) applies to nonplanar cases.

COMPARISON WITH EXPERIMENTAL RESULTS

In the remainder of this paper, experimental data will be presented and a comparison made with the predictions of sonic slender-body theory. Although these comparisons may not be ideal, since experimental data for $M_\infty=1$ are only available for families of shapes that strain the assumptions of the theory, they show remarkable agreement with the theory and help define the range for which the results may be expected to apply.

Cone-cylinders.—The most informative class of bodies to investigate further with regard to comparison of theory and experiment is the cone-cylinder. This is because of the availability of not only the similarity rules, etc., but also the complete solution for the pressure distribution and flow field in the vicinity of such bodies. Experimental data are also available in reference 18 by Solomon for the pressure at several points on the surface of two rather blunt circular cone-cylinders at Mach numbers near unity. The tests were conducted on cone-cylinders having semiapex angles of 20° and 25° and at Mach numbers up to about 0.96. The corresponding pressures at $M_\infty=1$ can be obtained only by extrapolation. The test Mach numbers are sufficiently high, however, that the local Mach numbers on the body surface are virtually independent of the free-stream Mach number. These pressures are plotted in figure 17 together with the theoretical pressure distribution for slender cone-cylinders at $M_\infty=1$. The latter were computed using equation (112) together with the theoretical pressure distribution for a circular cone-cylinder having semiapex angle $\theta=0.10$, see figure 9. With the exception of one point on the 25° cone-cylinder, the theoretical and experimental values are in remarkable agreement, considering the bluntness of the cones.

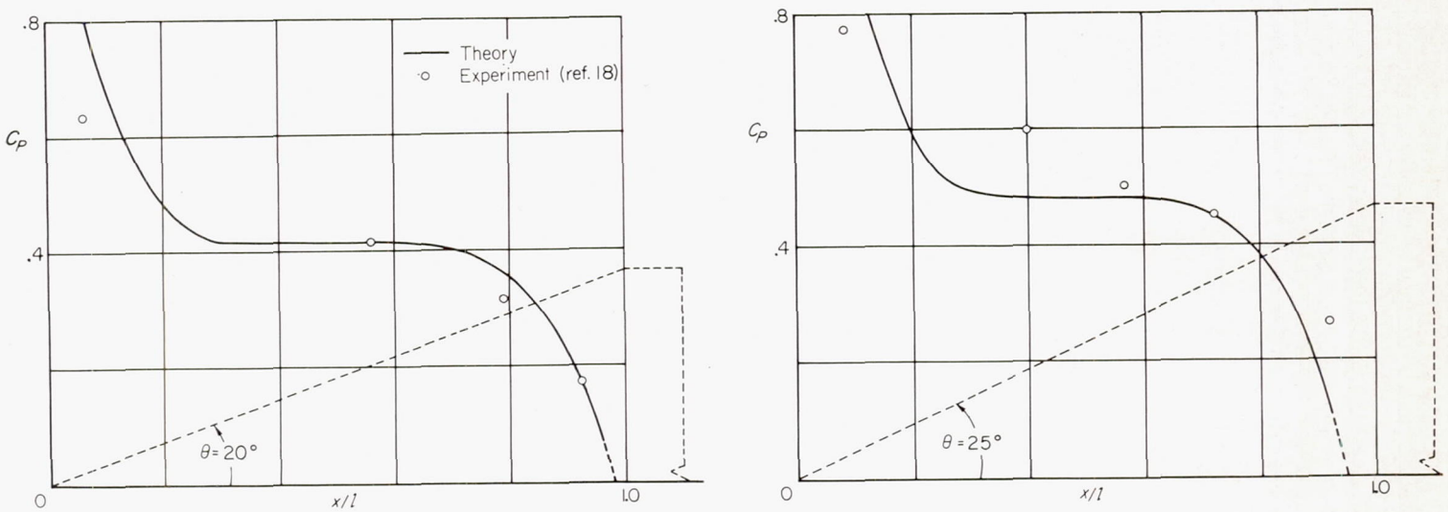

FIGURE 17.—Comparison of theoretical and experimental pressure distributions on two cone-cylinders at free-stream Mach number 1.

It would be very informative to make similar comparisons for cone-cylinders that are more slender, or that have noncircular cross sections, but the authors are unaware of any suitable experimental data. Studies involving bodies of revolution having area distributions that differ from that of cone-cylinders are handicapped at the present time by the lack of theoretical solutions for the transonic pressure distribution, and would have to be confined to the investigation of such items as the range of applicability of the similarity rules, the existence and lateral extent of the $g(x)$ function, etc.

Wings.—Since complete solutions for sonic flow around three-dimensional wings have not yet been obtained, the following discussion must be confined to cases in which experimental information is known for two or more wings or bodies having the same or affinely related longitudinal distributions of cross-section area. Probably the most extensive set of data of this type is that given in reference 20 for a large family of affinely related wings of rectangular plan form having NACA 63AOXX sections. Since the results for $M_\infty=1$ can be presented most concisely by using the variables suggested by the transonic similarity rules for wings of finite span (see, e. g., ref. 4), the experimental results for the zero-lift pressure drag and the lift-curve slope at $M_\infty=1$ are given in figure 18 by plotting $C_D/\tau^{5/3}$ and $\tau^{1/3}C_{L_\alpha}$ as functions of $A\tau^{1/3}$. As shown previously by McDevitt (ref. 20), these data confirm the statement provided by the similarity rules that the results so plotted should define a single curve for each aerodynamic quantity.

The curves representing the zero-lift pressure drag and the lift-curve slope have the same general form for high-aspect-ratio wings. The curves approach horizontal lines for the wings of larger aspect ratio, and the values for the lift and drag are not too different from the theoretical values given by Guderley and Yoshihara in references 30 and 31 for two-dimensional sonic flow around double-wedge profiles. The curves approach straight lines through the origin for low-aspect-ratio wings and the experimental values for the lift-curve slope of wings having $A\tau^{1/3}$ less than about unity practically coincide with the theoretical values given by

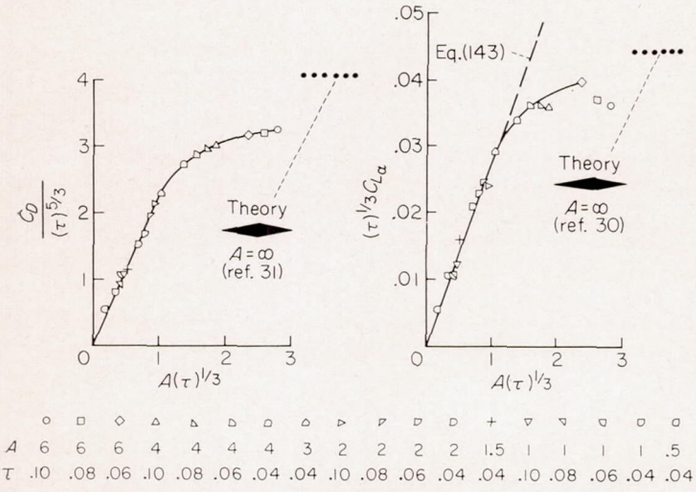

FIGURE 18.—Drag and lift at free-stream Mach number 1 of a family of rectangular wings having NACA 63AOXX profiles.

equation (143). The corresponding theoretical values for the drag at $M_\infty=1$ are not known.

Some measure of the applicability of the theoretical results can still be derived, however, by examining the relation between the experimental drags of various wings. If the effects of the violation of the theoretical requirements that occurs at the round nose of the unswept leading edge of each of the present family of wings can be disregarded, the discussion following equation (158) applies and all low-aspect-ratio wings having a given longitudinal distribution of cross-section area have the same drag. Inasmuch as not many pairs of wings of the present family actually have the same area distribution, a more useful statement of the result is that the drag is a unique function of the area distribution. Since the area distribution of an affinely related family of wings can be specified by giving, for instance, the chord l and the ratio S_m/l^2 (or its equivalent, the product of the aspect ratio and the thickness ratio) of the maximum cross-section area to the chord squared, it follows that the drag and geometry of the present family of wings are related according to

$$\frac{D}{(\rho_\infty U_\infty{}^2/2)l^2}=f_1\left(\frac{S_m}{l^2}\right)=f_1(A\tau) \tag{161}$$

where f_1 represents an unknown function of the indicated variables. This relation may be contrasted with that provided by the similarity rule that states

$$\frac{C_D}{\tau^{5/3}}=\frac{D}{(\rho_\infty U_\infty{}^2/2)S_p\tau^{5/3}}=f_2(A\tau^{1/3}) \tag{162}$$

where S_p refers to the plan-form area. At first glance, the two relationships appear to bear only slight resemblance. It can be seen upon closer examination, however, that some of the apparent differences are superficial and of little or no significance. Thus, let equation (161) be rewritten as

$$D=\frac{\rho_\infty U_\infty{}^2}{2}\,l^2f_1(A\tau)=\frac{\rho_\infty U_\infty{}^2}{2}\,\frac{S_p}{A}\,(A\tau)^2f_3(A\tau)$$

or

$$\frac{C_D}{\tau^{5/3}}=A\tau^{1/3}f_3(A\tau) \tag{163}$$

This appears to be the closest that the two results can be brought together without introducing additional restrictions or approximations. Both are now concerned with the same quantity, $C_D/\tau^{5/3}$, but equation (162) states that this quantity is equal to some unknown function of $A\tau^{1/3}$, whereas equation (163) states that it is equal to $A\tau^{1/3}$ times some function of $A\tau$. The only way in which both results can be universally correct is for the functions f_2 and f_3 to be constants and not dependent on either $A\tau$ or $A\tau^{1/3}$. Both rules are not universally correct, however, since equation (163) is derived from transonic slender-body theory and therefore can be expected to apply only to wings of small aspect ratio. From the foregoing considerations, one can conclude that the drag at $M_\infty=1$ of the low-aspect-ratio wings of the present family must depend on the geometry in such a way that $C_D/\tau^{5/3}$ is linearly proportional to $A\tau^{1/3}$. Examination of the drag data of figure 18 shows that the experimental results exhibit precisely this trend for wings of $A\tau^{1/3}$ less

than about unity. An alternative interpretation of this result is that the drag of a number of low-aspect-ratio wings of the present family all having the same chord, varies as the square of the frontal area; that is, $D\Big/\left(\frac{1}{2}\rho_\infty U_\infty{}^2 l^2\right)$ depends on the square of S_m/l^2. Further discussion of these and related points appears in reference 32.

It appears that the degree of correspondence between theory and experiment disclosed above for such extreme cases as rectangular wings of aspect ratios 3 and 4 must be attributed partially to the averaging influence of integration and that the same close correspondence may not be found for more detailed quantities. For example, slender-body theory indicates that the lift on low-aspect-ratio rectangular wings at $M_\infty=1$ is concentrated along the leading edge. Although pressure-distribution measurements were not included in the test program reported in reference 20, pitching-moment measurements were made from which the center-of-pressure position can easily be deduced. The results indicate that the center-of-pressure position at small angles of attack is within the first 10-percent chord at $M_\infty=1$ for each of the wings of aspect ratio 1/2 or 1, but moves progressively rearward for wings of larger aspect ratio. Hence the range of $A\tau^{1/3}$ for which theory and experiment agree may be expected to be less than that indicated by the integrated lift and drag results. On the other hand, application to wings of the rectangular plan form imposes severe strain on the slender-body assumptions, and better agreement, or a wider range of applicability, might be anticipated with wings of other plan form, such as triangular.

Wing-body combinations.—Several comparisons between the experimental zero-lift drags of wing-body combinations and bodies of revolution having the same longitudinal distribution of cross-section area were given by Whitcomb in reference 6 in connection with his discovery of the area rule. The bodies tested were of such geometry that the integrals of equation (153) are zero and the drags of wing-body combinations and their equivalent bodies of revolution should be the same. The experimental results show excellent agreement in some cases, and lesser agreement in other cases. These results will not be discussed further here since the experimental data are already analyzed from the point of view of equality of drag in reference 6.

Ames Aeronautical Laboratory
National Advisory Committee for Aeronautics
Moffett Field, Calif., *Apr. 2, 1956*

REFERENCES

1. Spreiter, John R.: Theoretical and Experimental Analysis of Transonic Flow Fields. NACA—University Conference on Aerodynamics, Construction, and Propulsion. Vol. II, Aerodynamics. A compilation of the papers presented, Lewis Flight Propulsion Laboratory, Cleveland, Ohio, Oct. 20–22, 1954.
2. von Kármán, Theodore: The Similarity Law of Transonic Flow. Jour. Math. Phys., vol. XXVI, no. 3, Oct. 1947, pp. 182–190.
3. Berndt, Sune B.: Similarity Laws for Transonic Flow Around Wings of Finite Aspect Ratio. KTH-Aero. TN 14, Roy. Inst. Tech., Division of Aeronautics, Stockholm, Sweden, 1950.
4. Spreiter, John R.: On the Application of Transonic Similarity Rules to Wings of Finite Span. NACA Rep. 1153, 1953. (Formerly NACA TN 2726)
5. Oswatitsch, Klaus, and Berndt, Sune B.: Aerodynamic Similarity at Axisymmetric Transonic Flow Around Slender Bodies. KTH-Aero TN 15, Roy. Inst. Tech., Division of Aeronautics, Stockholm, Sweden, 1950.
6. Whitcomb, Richard T.: A Study of the Zero-Lift Drag-Rise Characteristics of Wing-Body Combinations Near the Speed Sound. NACA RM L52H08, 1952.
7. Oswatitsch, Klaus: Die theoretischen Arbeiten über schallnahe Strömunger am Flugtechnischen Institut der Kungl. Tekniska Högskolan, Stockholm. Proc. of Eighth Int. Cong. on Theo. and Appl. Mech., 1953, pp. 261–262.
8. Oswatitsch, Klaus, and Keune, Friedrich: Ein Äquivalensatz für nichtangestellte Flügel kleiner Spannweite in schallnaher Strömung. Zeitschrift für Flugwissenschaften, 3 Jahrgang, Heft 2, Feb. 1955, S. 29–46.
9. Oswatitsch, Klaus: Die Geschwindigkeitsverteilung bei lokalen Überschallgebieten an flachen Profilen. Zeitschrift für Angewandte Mathematik und Mechanik. Bd. 30, Heft 1/2, Jan./Feb., 1950, S. 17–24.
10. Oswatitsch, Klaus: Die Geschwindigkeitsverteilung an symmetrischen Profilen beim Auftreten lokaler Überschallgebiete. Acta Physica Austriaca, Bd. 4, Nr. 2–3, Dec. 1950, S. 228–271.
11. Gullstrand, Tore R.: The Flow Over Symmetrical Aerofoils Without Incidence in the Lower Transonic Range. KTH-Aero. TN 20, Roy. Inst. Tech., Division of Aeronautics, Stockholm, Sweden, 1951.
12. Gullstrand, Tore R.: The Flow Over Symmetrical Aerofoils without Incidence at Sonic Speed. KTH-Aero. TN 24, Roy. Inst. Tech., Division of Aeronautics, Stockholm, Sweden, 1952.
13. Gullstrand, Tore R.: A Theoretical Discussion of Some Properties of Transonic Flow Over Two-Dimensional Symmetrical Aerofoils at Zero Lift with a Simple Method to Estimate the Flow Properties. KTH-Aero. TN 25, Roy. Inst. Tech., Division of Stockholm, Sweden, 1952.
14. Gullstrand, Tore R.: The Flow Over Two-Dimensional Aerofoils at Incidence in the Transonic Speed Range. KTH-Aero. TN 27. Roy. Inst. Tech., Division of Aeronautics, Stockholm, Sweden, 1952.
15. Spreiter, John R., and Alksne, Alberta: Theoretical Prediction of Pressure Distributions on Nonlifting Airfoils at High Subsonic Speeds. NACA Rep. 1217, 1955. (Formerly NACA TN 3096)
16. Harder, Keith, and Klunker, E. B.: On Slender-Body Theory at Transonic Speeds. NACA RM L54A29a, 1954.
17. Yoshihara, Hideo: On the Flow Over a Cone-Cylinder Body at Mach Number One. WADC Tech. Rep. 52–295, 1952.
18. Solomon, George E.: Transonic Flow Past Cone Cylinders. NACA TN 3213, 1954.
19. Heaslet, Max. A., Lomax, Harvard, and Spreiter, John R.: Linearized Compressible-Flow Theory for Sonic Flight Speeds. NACA Rep. 956, 1950.
20. McDevitt, John B.: A Correlation by Means of Transonic Similarity Rules of Experimentally Determined Characteristics of a Series of Symmetrical and Cambered Wings of Rectangular Plan Form. NACA Rep. 1253, 1955.
21. Bateman, H.: Partial Differential Equations of Mathematical Physics. Dover Pub., N. Y., 1944.
22. Heaslet, Max. A., and Lomax, Harvard: The Use of Source-Sink and Doublet Distributions Extended to the Solution of Boundary-Value Problems in Supersonic Flow. NACA Rep 900, 1948.
23. Heaslet, Max. A., and Lomax, Harvard: Further Remarks Concerning Integral Transforms of the Wave Equation. Jour. Aero. Sci., vol. 21, no. 2, Feb., 1954, p. 142.
24. Volterra, V.: Lecons sur L'integration des Equations Differentielles aux Derivees Partielles. Herman et Fils. Paris, 1912.

25. Heaslet, Max. A., and Lomax, Harvard: Supersonic and Transonic Small Perturbation Theory. Sec. D of General Theory of High Speed Aerodynamics. Vol. VI of High Speed Aerodynamics and Jet Propulsion, W. R. Sears, ed., Princeton Univ. Press, 1954.
26. Guderley, G., and Yoshihara, H.: An Axial-Symmetric Transonic Flow Pattern. Quart. Appl. Math., vol. 8, no. 4, Jan. 1951, pp. 333–339.
27. Heaslet, Max. A., and Lomax, Harvard: The Calculation of Pressure on Slender Airplanes in Subsonic and Supersonic Flow. NACA Rep. 1185, 1954.
28. Jones, Robert T.: Leading-Edge Singularities in Thin-Airfoil Theory. Jour. Aero. Sci., vol. 17, no. 5, May 1950, pp. 307–310.
29. Berndt, Sune B.: On the Drag of Slender Bodies at Mach Number One. Zeitschrift für angewandte Mathematik und Mechanik. Bd. 35, Heft 9/10, Sept./Okt. 1955, S. 362.
30. Guderley, Gottfried, and Yoshihara, Hideo: Two-Dimensional Unsymmetric Flow Patterns at Mach Number 1. Jour. Aero. Sci., vol. 20, no. 11, Nov. 1953, pp. 757–768.
31. Guderley, Gottfried, and Yoshihara, Hideo: The Flow Over a Wedge Profile at Mach Number 1. Jour. Aero. Sci., vol. 17, no. 11, Nov. 1950, pp. 723–735.
32. Spreiter, John R.: On the Range of Applicability of the Transonic Area Rule. NACA TN 3673, 1956 (Formerly NACA RM A54F28).

U. S. GOVERNMENT PRINTING OFFICE: 1957